Dam Break Risk Assessment in Baker Valley (Chilean Patagonia)

by

Elisabetta Natale

B.S. Civil and Environmental Engineering
Università di Pavia, 2007

SUBMITTED TO THE DEPARTMENT OF CIVIL AND ENVIRONMENTAL ENGINEERING IN PARTIAL FULFILLMENT OF THE REQUIREMENTS FOR THE DEGREE OF

MASTER OF ENGINEERING IN CIVIL AND ENVIRONMENTAL ENGINEERING
AT THE
MASSACHUSETTS INSTITUTE OF TECHNOLOGY

JUNE 2009

Signature of Author:

_____

Department of Civil and Environmental Engineering
May 8, 2009

Certified by:

_____

Dara Entekhabi
Professor of Civil and Environmental Engineering
Thesis Supervisor

Accepted by:

_____

Daniele Veneziano
Chairman, Departmental Committee for Graduate Students

Dam Break Risk Assessment in Baker Valley (Chilean Patagonia)

by

Elisabetta Natale

B.S. Civil and Environmental Engineering
Università di Pavia, 2007

Submitted to the Department of Civil and Environmental Engineering
on May 8, 2009 in Partial Fulfilment of the Requirements for the Degree of
Master of Engineering in Civil and Environmental Engineering

ABSTRACT

An hydroelectric project was proposed by HidroAysén Company in the Aysén Region of Chilean Patagonia. It consisted of the installation of five hydroelectric power stations, two on Rio Baker and three on Rio Pascua, with an average annual energy production of 18,430 GWH. The Environmental Impact Assessment (EIA) presented by HidroAysén lacked of a dam failure impact assessment, crucial to prevent or minimize the impact of unexpected flooding caused by a dam failure.

A dam break risk assessment was performed for the so called Baker 2, a proposed concrete gravitational dam located on the Rio Baker, upstream the small community of Caleta Tortel, an area of concern for potential flooding.
Using ORSA Code, software developed by a research collaboration between the University of Pavia and the University of Rome - La Sapienza (Italy), a computational model was performed to simulate the flood wave propagation associated with a dam break failure scenario. The areas subject to flooding were mapped on the digital elevation model (DEM) of the surface topography.

Thesis Supervisor: Dara Entekhabi
Title: Professor of Civil and Environmental Engineering

1. Project Overview

Background[1]

1.1 Location

Chile is a South American country flanked by Argentina and Bolivia to the East, Peru to the North, and the Pacific Ocean to the West. With a total area of 757,000 sq km, Chile is approximately twice the size of Montana. Because of its unique geography spanning from approximately -20° to -56° latitude, Chile's climate varies greatly. Generally temperate, the climate can be characterized as desert in the north, Mediterranean in the central region, and cool and damp in the south (CIA, 2008). Chile's terrain is as varied as its climate with a combination of low coastal mountains, a fertile central valley, and the rugged Andes in the east. (
Figure 1)

Figure 1 – Map of Chile (source: www.southwindadventures.com)

[1] From "Analysis of proposed hydroelectric dams in Chilean Patagonia", Kristen Burrall, Gianna Leandro, Laura Mar, Elisabetta Natale, Flavia Tauro, MIT, USA.

The 10 million-hectare Aysén Region is home to the Rio Baker and is Chile's least populous administrative region with approximately 0.9 person/sq km (personal communication). With such a low population density, the region is a prime example of pristine natural conditions. The watershed that contains the Rio Baker encompasses a wide variety of habitats from mountain glaciers to river-braided floodplains, and in these varied physical habitats a large array of plant and animal species thrive (Strittholt, 2008). The Rio Baker is a 170 km river which originates in Bertrand Lake and empties into the fjords of the Pacific Ocean near the small community of Tortel.

Due to the remote location of the Rio Baker watershed few studies have been conducted as to the potential impacts of dam installation on the region's biology and ecology (Strittholt, 2008). Accordingly, this paper elucidates the key impacts of the dams in an approach that combines various research objectives through a systematic evaluation.

1.2 Water Rights

Currently, water rights in Chile are privatized under a system of water law similar to that of the Western United States (personal communication). Endesa Spain, one of the largest electrical companies in the world, controls more than 80% of the water rights on the Rio Baker and, with this jurisdictional freedom, Endesa endeavors to install two hydroelectric dams on the river. There are a host of proponents for and opponents against the dams. Proponents argue that the dams will help secure Chile's energy independence, create jobs, and provide power for the mining industry that supports the Chilean economy, whereas opponents argue that the dams will irreparably destroy natural habitats while simultaneously increasing energy costs for Chileans (personal communication).

1.3 Energy Demand

Electricity demand in Chile centers on Santiago and the nation's mining industries (personal communication). Increased GDP and transport in Chile have heightened energy demand throughout the country and especially in the northern regions. Installing the dams will address this increased demand. The combined capacity of the project will total 2,750 megawatts, approximately 20% of Santiago's current energy demand. This electricity will be transported northward from the Aysén Region to Santiago via 2,240 km of transmission lines, which require a 92-meter wide clear-cut swath through 14 national parks (International Rivers, 2008). In addition to supplying Santiago and industry with electricity, the dams are a step toward increasing Chile's domestic energy security.

1.4 Proposed Hydroelectric Project

HidroAysén is a joint venture between Endesa Chile, a Spanish energy company, and Colbun S.A., a Chilean electricity generation company (HidroAysén, 2007). The

1.4 Proposed Hydroelectric Project

HidroAysén is a joint venture between Endesa Chile, a Spanish energy company, and Colbun S.A., a Chilean electricity generation company (HidroAysén, 2007). The HidroAysén project consists of five hydroelectric dams on two rivers: the Rio Baker and the Rio Pascua. The combined capacity of the dam system would generate, on average 18,430 GWh of power annually, the equivalent of 30% of the power currently installed in the Central Interconnected System (SIC) grid. Power generated by the dams connect through local transmission lines, long distance high voltage transmission lines will connect the dams, which are in the Aysén grid to the SIC (HidroAysén, 2008). If constructed, the five dams will inundate 5,910 hectares; further, dam construction and operation will disturb an additional 11,000 hectares.

A local electricity grid will combine the output from the five dams and will convert alternating current (AC) to direct current (DC) for long distance transmission (HidroAysén, 2008). The 2,240 km transmission line will require five thousand 50-meter towers spaced 400 meters apart through a 70-meter easement (Patagonia without Dams Campaign). Since generation, transmission and distribution under Chile's *General Law of Electrical Services*, Transelec will design the high voltage transmission line separately from the HidroAysén dams. CONAMA, Chile's equivalent of the United States' Environmental Protection Agency, will evaluate the environmental impact of the dams and the transmission lines separately. The transmission lines are a great source of controversy. One question surrounds the total capacity of the DC line: if their capacity is greater than the 2750 MW that the HidroAysen dam project would provide, will other hydroelectric developments follow?

2. Glacial-Lake Outburst Floods (GLOFs)

The recent global climatic change has brought a tremendous impact on the high mountainous glacial environment. Many of the big glaciers melted rapidly and gave birth to the origin of a large number of glacier lakes. GLOFs are not a new phenomenon but with the worldwide receding of glaciers and rising temperature, the probability of their occurrences has dramatically risen.

As glaciers retreat, glacial lakes form behind moraine or ice 'dams'. These 'dams' are comparatively weak and can breach suddenly, leading to a discharge of huge volumes of water and debris. Such outbursts have the potential of releasing millions of cubic meters of water in a few hours causing catastrophic flooding downstream.

A lake outburst can be triggered by several factors: ice or rock avalanches, the collapse of the moraine dam due to the melting of ice buried within, the washing out of fine material by springs flowing through the dam (piping), earthquakes or sudden inputs of water into the lake e.g. through heavy rains or drainage from lakes further upglacier.

Many researchers have demonstrated that infrequent, large magnitude floods in mountain environments are significant geomorphic agents because only these floods are capable of generating the hydraulic forces necessary to entrain and transport the large material that constitutes the channel and valley bottom in these regions.

Erosional and depositional features produced by GLOF vary longitudinally along the flood routes as complex interactions between flood hydraulics, boundary conditions, sediment supply, and the temporal sequence and magnitude of past floods. Figure 2

The large-scale erosional and depositional features created by an extreme flood in mountainous environments are typically persistent features that remain unaltered because normal floods are not able to rework the coarse sediments (Cenderelli et al. 2003).

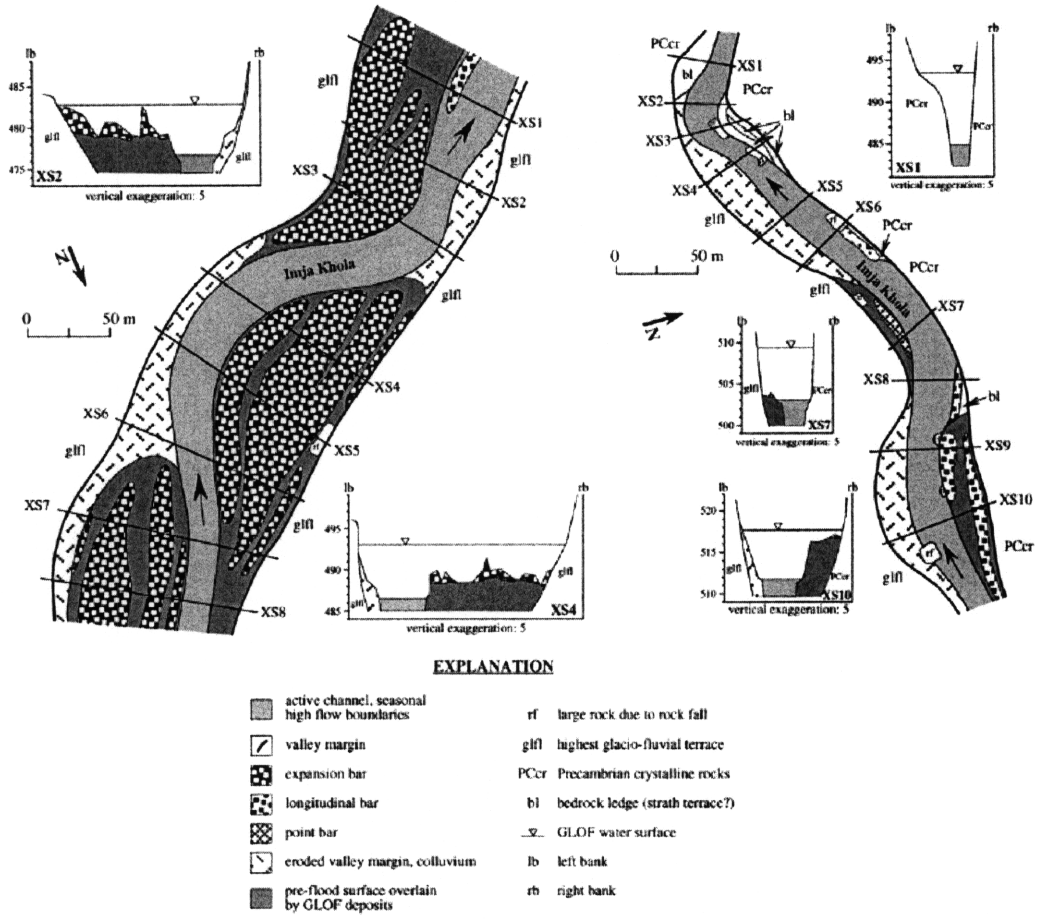

Figure 2- Geomorphic maps showing the distribution of erosional and depositional features produced by a GLOF. For the cross-sections, the elevations are relative and in units of metres (after Cenderelli and Wohl, 2001. Reprinted with permission from Elsevier Science).

A GLOF might be modelled as a shallow water surface wave generated by landslides.

In such events the primary risk is not associated with the sliding mass but instead to the waves generated by the energy transferred to the water by the collision. A secondary risk is the possibility of large scale deposition of material on the river bed forming an artificial dam able to accumulate a large amount of water temporarily, giving rise to further catastrophic dam failure. (Perez et al. 2006).

An appropriate numerical method could be based on Roe's approximate Riemann solver (see §6.1.4), as ORSA code one. Moreover a recent study demonstrates that one-dimensional modelling of GLOF propagation provides results broadly comparable to data derived from more complex simulations. (Petteri et al. 2007).

Although the enormous numbers of limitations of a GLOF study, the results of a hydrodynamic modelling can be a cost-effective.

The vulnerability maps generated through such tool provide a scientific basis for identifying who is vulnerable and which infrastructure and agricultural land is most likely to be affected. This information can be of great value in developing better options for management plans and their implementation. (Bajracharya et al. 2007).

2.1 *GLOF Frequency in the Aysén Region of Chilean Patagonia*

Until April 2008, no GLOF events had been recorded in the Northern Patagonian Icefield (NPI). Since that year, this phenomenon has occurred four times so far. Lago Cachet 2, a 5 square kilometer-wide and 100 meter-deep glacial lake near the snout of the Colonia Glacier, has created a GLOF by emptying its volume through a system of 8 km long tunnels. The water has been released into Lago Colonia which feeds Rio Colonia. Lago Colonia's increase in water level was not significant: it discharged the excess water into the Rio Baker.

The effect of a GLOF into the Rio Baker results into an increase of the water level and an associated water temperature drop (Table 1).

		Apr-07-2008	Diff.	Oct-08-2008	Diff.	Dec-22-2008	Diff.	Mar-05-2009	Diff.
Q (m^3/s)	max	3'575	303%	3'007	561%	3'052	291%	3'812	324%
	average	1'181		536		1'048		1'176	
Water Level (m)	max	6.71	241%	5.85	522%	5.92	235%	7.06	254%
	average	2.79		1.12		2.52		2.78	
Temperature (°C)	minimum	4.6	53%	4.5	62%	8.1	74%	3.8	36%
	average	8.6		7.3		10.9		10.5	

Table 1 – Summary of recent GLOFs (Q, water level, water T) with a comparison between peak values and base values

A possible explanation for the sudden occurrence of these events can be found in the climate change that this area has experienced in the last four decades. Meteorological stations in the Aysén region have recorded a half-degree increase in temperature since the early 1970s. At the same time, precipitation is decreasing, causing diminished ice formation. Glacial systems are based on an equilibrium that is very sensitive to climate fluctuations. The NPI is a temperate glacier that contains ice below the melting temperature throughout its mass. Ice formation occurs only in

winter and it is a result of snow compaction. If precipitation decreases and temperature increases, the rate at which the glacier melts will be faster than the rate at which ice is formed. This produces a mass shrinkage. The Colonia Glacier has been shrinking since the last decade but this fact has not produced visible results until the outburst occurred.

With respect to Lago Chachet 2 GLOFs, the increase in temperature has led to multiple effects:

- *Ice melting*. The responsible is the increased temperature of the air that has allowed the melting of the glacier and consequently the formation and filling of Lago Cachet 2.
- *Bank thinning*. Due to the double action of the air and lake temperature (that reflects the climate change as well), the banks of Lago Cachet 2 have reduced as well and the ice overburden is significantly decreased.
- *Tunnel formation*. The fractures already present in the glacier have probably formed larger and interconnected moulins that, under the effect of the warmer lake temperature during the outbursts, have continued to grow and to let the drainage of the lake itself.

The role of the air temperature is particularly relevant for the frequency of the outburst: the rate at which Lago Cachet 2 is filled is a consequence of the warming trend.

While the peak runoff of each recent GLOF event was almost constant, the trend is alarming. In fact, the time between events has decreased along a geometric progression.

3. Dam Failure Impact Assessment

The dam-break inundation zone is defined as the area downstream of a dam that would be inundated or otherwise directly affected by the failure of a dam.

The simulation of dam breach events and the associated flooded area are crucial to reduce threats from unexpected flooding caused by a dam failure and are often required by State's legislation and technical regulation. The dam failure impact assessment would determine whether the dam is a referable dam, if there is a danger of the dam failing and which action is necessary to prevent or minimise the impact of the failure.

Although it seems that the Chilean law doesn't include any dam's safety regulation, a massive dam project should be supported by a complete flood risk assessment.

Dam-break studies are not only achieved to pursue safety legislation, often lacking, but they are frequently commissioned by the dam owners in order to avoid the costly upgrades to their dam to meet increased dam safety standards that are applied as a result of the downstream development.

The dam failure assessment procedures here presented follows the guideline published by the Department of Natural Resources and Mines of the Queensland Government, Australia (2002).

Guidelines

The methodology of dam failure impact assessment should require the following activities:

- Inspection of dam site
- Accurate collection of data
- Identification of flood prone areas
- Identification of population at risk
- Certification of a final written dam failure impact assessment by a registered professional engineer and submission to the chief executive.

3.1 Dam Site Inspection

Site inspections are mandatory and ensure that the information upon which the dam failure impact assessment is based is correct and up-to-date, and also enable an

appreciation of the characteristics of the site. Site inspections must include areas that could be affected by dam failure both upstream and downstream of the dam.

Site inspections are needed to:

- Verify the accuracy of all mapping/aerial photogrammetry that is used in the assessment
- Verify the existence of buildings and other places of occupation to justify the failure impact rating identified in the assessment
- Identify other storages on the same waterway
- Identify buildings and other places of occupation along waterways, which may house population at risk
- Identify catchment modification works (e.g. diversion drains and levee banks).

3.2 Data Collection

The appropriateness and accuracy of the information included in the assessment must be judged by the engineer that certifies the failure impact assessment. A wide array of information needs to be collected to determine the effects of a dam failure. These include:

3.2.1 General Information

Floods related to dam failure are generally significantly larger than natural floods. Information that should be included in the assessment is:

- Available historic flood levels
- Hydrographic data
- Rainfall/runoff model results
- Dam break flood model results under "sunny day" and "incremental" conditions.

3.2.2 Dam and storage information

The information used to determine potential breach characteristics and incremental flooding effects should include:

- Type of dam and location (including latitude and longitude)

- Spillway type and adequacy (including flood control facilities such as gates and secondary spillways)
- Dimensions such as height and length of embankments and the width of the crest
- Storage capacity to full supply level and to the crest of the dam (stage capacity curve)
- Use of dam including contents of the storage area
- Possible causes and modes of failure
- Comments on design, foundations and any unusual conditions
- Design studies or reports.

Additional pieces of information should regard the stability of slopes and earthquake effects.

3.2.3 Topographic information

Sufficient topographic information must be obtained to accurately determine:

- The shape and slope of the valley downstream of all potential failure locations
- Controls on the downstream flow (i.e. culverts, vegetation, weirs, bridges, embankments, surface roughness and temporary storage on the flood plains)
- Location of major downstream tributaries.

If regional maps do not provide sufficient detail for a failure impact assessment, further information may need to be obtained from sources such as:

- Road maps
- Orthographic, topographic, military and cadastral plans
- Surveyed cross-sections
- Aerial photographs
- Satellite imagery
- Local residents.

It is important to note that mapping or aerial photogrammetry may not contain recent developments e.g. houses or other places of occupation. Information contained in photogrammetry that plays an integral role in the assessment must be verified by site inspections.

Where extreme precision is required, extensive, detailed surveys of the downstream valley may be necessary. In such circumstances, surveys may also be required to locate and determine natural surface levels at all buildings or other places of occupation that are thought to be at risk.

3.2.4 Hydrographic data

The results of a dam-break analysis will depend on a number of parameters such as:

- The size of the available flood storage
- The height of the dam
- The size and capacity of its spillway
- The shape of the valley downstream of the dam.

For an accurate dam-break analysis, the values of the Manning roughness coefficient[2] should be varied in each cross-section according to the local survey. For lower accuracy analyses, only one roughness coefficient might be sufficient in representing the whole floodplain.

Where previous flood records exist in the river or stream reach under consideration, the hydraulic model should be calibrated to match the available flood inundation data so that the numerical dam-break model can be demonstrated to approximate actual flow conditions. If these records are not available, or are available for a limited range of flows, some assessment must be made of the potential impact on the accuracy of the modelled results. All modelling must be subjected to sensitivity analyses to test sensitivity to model assumptions.

3.2.5 Hydrologic data

Downstream tributary inflows may impact on the dam break flood, particularly if population centres are some distance downstream of the dam. Simpler analyses on smaller dams would not normally consider inflows from tributaries downstream of the dams.

[2] The Manning coefficient is a roughness parameter used to model energy losses in streams. Unless reasonable discharge and water level calibration is available, reference should be made to standard hydraulic engineering texts for appropriate values of the parameter.

3.2.6 Downstream community information

Downstream community information must include the location, number and nature of buildings, other places of occupation and approved camping and recreational areas in the failure impact zone.

This information may be obtained from maps, persons with local knowledge and emergency action plans for the dam. Recent aerial photogrammetry also provides useful information on the location of downstream structures. As stated above, site inspections must be undertaken to verify downstream community information (for example, to ensure the information is up to date and identifies buildings and other places of occupation obscured by trees).

3.2.7 Determination of Flood Prone Areas

The flood prone area, defined as the failure impact zone, is the area affected by flooding as a result of a major flood event, e.g. the failure of the dam. Failure impact zones must be determined for all failure events specified within the analytical technique used for the failure impact assessment and for all other failure events relevant to the dam.

It should be noted that while the dam failure impact zone is generally located downstream, areas upstream can also be affected and should be included where relevant (e.g. an upstream area may be affected by the abnormal operation of discharge control devices such as gates or inflatable bags).

A map showing the extent of the flood prone areas must be included in the written assessment.

3.2.8 Population at risk

People are considered part of the population at risk if buildings or any part of the ground where these buildings are located lie within the failure impact zone.

When the failure impact zone is being determined, the number, location and nature of buildings and other places of occupation must be identified.

The population at risk is the difference between the population at risk for a specific dam failure and the population at risk from the natural flooding even if dam failure does not occur.

Dam failure during a flood: some people could be at risk from the natural flooding even if dam failure does not occur.

Figure 3)

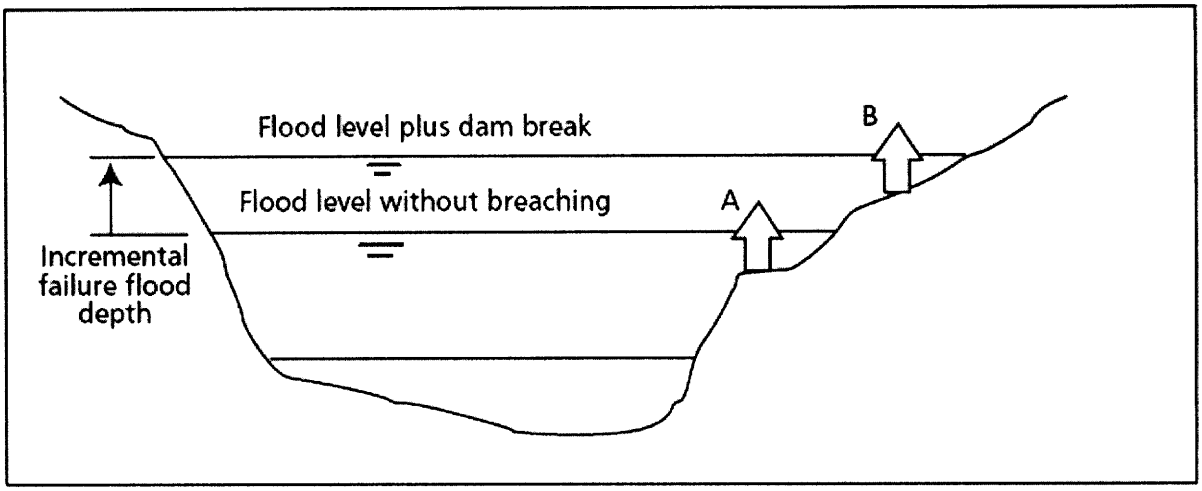

Figure 3 – Dam failure during a flood. (Guidelines for Failure Impact Assessment of Water Dams, State of Queenland, 2002)

A 'sunny day' dam failure (when flooding is due to dam failure only): nobody is at risk if the dam does not fail.

Figure 4)

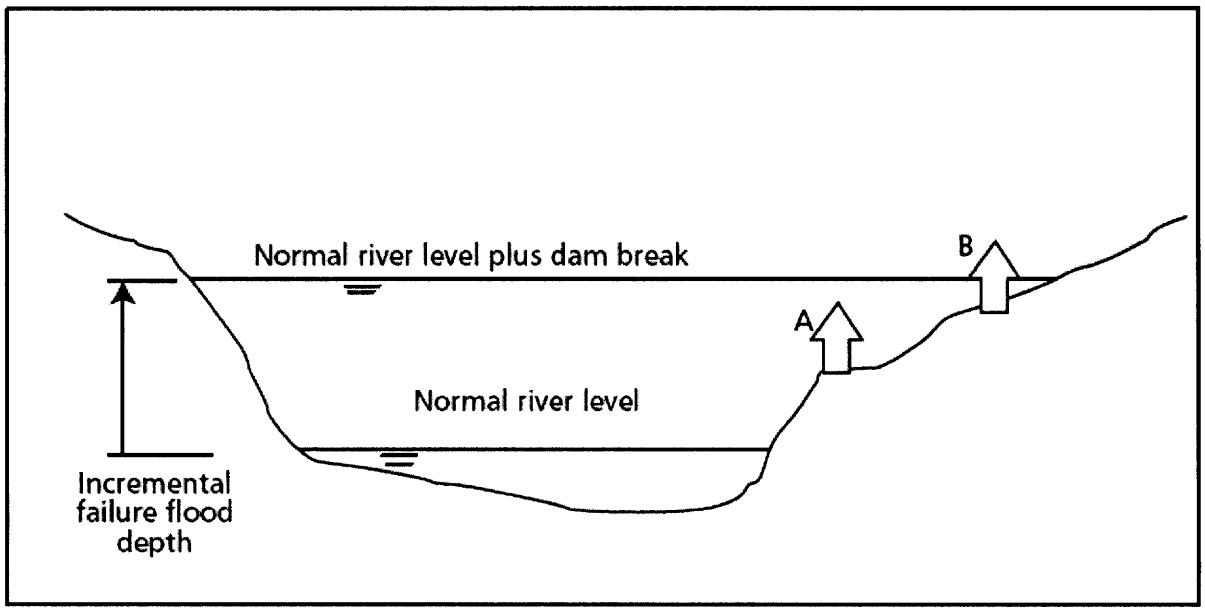

Figure 4 – Sunny day dam failure

3.3 *Accuracy of population at risk calculations*

A variety of factors may affect the accuracy of population at risk calculations. These must be considered to ensure the reliability of population at risk calculations. Factors include:

- The accuracy of cross-sections used in the analysis
- The locations of cross-sections used in the analysis
- The accuracy of the hydraulic modelling
- Availability and accuracy/reliability of calibration data and the degree of extrapolation required to model dam break flows
- Assumed hydraulic roughness parameters
- Assumed breach development times
- Locations, numbers and elevations of buildings and other places of occupation.

The degree of conservativeness should reflect the amount of calibration data available to determine stream channel roughness for the watercourse reaches in question.

The written dam failure impact assessment should include a statement on the range of the estimate of population at risk for the critical case. Such an assessment should indicate values for the upper limit of population at risk that could reasonably be expected as a result of the analysis and a similarly derived lower limit of population at risk.

3.4 *Analytical Techniques*

Three analytical techniques may be used in preparing dam failure impact assessments. These are two-dimensional flow analysis, simplified assessment techniques and comprehensive assessment techniques. These techniques may be used alone or in combination. Certifying registered professional engineers need to be satisfied that the techniques selected and the accuracy of the models developed are reasonable for the situations under consideration.

3.4.1 Two-dimensional flow analysis

This analysis will typically need to be used if the population is situated in a risk location close to a possible dam breach and there is a risk that the population will be flooded.

Models used in such analyses need to be able to simulate the dynamic behaviour of overland flow over complex geometries, determining inundated areas for two-dimensional flows.

3.4.2 Simplified assessment

A simplified dam failure impact assessment technique may be justified where there is little doubt as to the population at risk and the cost of a comprehensive assessment is anticipated to be high relative to the potential benefits. It involves the conservative use of topographic and hydrographic data and an empirically determined breach discharge.

This is an approximate technique, which uses the 'normal' depth at a section to estimate maximum flood levels at a point for a given discharge. As such this technique does not take any backwater effects into account. It must not be used where backwater effects are expected to be significant in terms of the affected population at risk. Aside from the backwater effects, the principal areas of uncertainty are the accuracy of the stream slopes, the cross-sections, and the locations and levels of the impacted buildings.

The maximum breach discharge from a dam during a breaching event is typically determined using empirical relationship based on statistical analysis of previous dam failures.

3.4.3 Comprehensive assessment

If a simplified assessment is not accurate enough to adequately calculate the population at risk, then a comprehensive dam break analysis may be required. A comprehensive assessment is a detailed assessment of the failure impact zone and the population at risk if the dam fails. Dam break analyses must be undertaken for a range of dam failure scenarios and use current hydraulic modeling practice and suitably documented and validated numerical models.

Some estimate of the accuracy of each numerical model used for the dam-break analysis must be made and this accuracy must be taken into account in assessing potential population at risk as indicated in the previous sections. The impact on population at risk will be greatest in areas with higher populations (e.g. towns), and it may be justified to selectively improve accuracy in these areas.

3.4.4 Two or more dams on the same watercourse

Sometimes, two or more dams occur on the same watercourse. In such circumstances, it must be assumed that the failure of an upstream dam may trigger

the failure of downstream dams. If the downstream dam cannot store the contents of the upstream dam without failure, the combined effect of multiple dam failures must be considered when determining the incremental population at risk for the upper dam for failure events. Similarly, if failure of a downstream dam could contribute to the failure of an upstream dam (such as through a rapid drawdown failure if headwaters of the downstream dam back up against the upstream dam), the potential failure of the upper dam must be considered when determining the incremental population at risk of the lower dam for failure events.

The dam failure case producing the highest incremental population at risk must be used to determine the failure impact rating for the dam.

3.4.5 Other failure events

If the registered professional engineer considers that other failure events could result in a higher incremental population at risk, these failure conditions must be considered and described in the written dam failure impact assessment. These failures may include:

- Storage rim instability.
- Factors such as deterioration, old age, design or construction faults and poor maintenance.
- Damage due to fire, wind and escape of water into mining tunnels/shafts beneath reservoirs.
- Vandalism.

3.5 Periodic Re-Assessment of Failure Impact Rating

The dam owners should provide a periodic re-assessment of the dam failure including whether or not there has been substantial changes in:

- the stream channel cross-sections and roughness
- the embankment and spillway geometry
- the magnitude of the design floods
- the downstream population

The population at risk must be re-calculated as part of each re-assessment of the failure impact rating.

4. Case study

The dam-break analysis hereafter described is supplying, although in a small portion, the total absence of a dam failure safety assessment into the EIA presented by Endesa.

The starting case study of the analysis consisted of the simulation of a recent Glacial Lake Outburst Flood (GLOF) event. This first step allowed to calibrate the model comparing the mathematical results of the software with the real data collected during the event. Furthermore, the analysis gives an additional insight on the GLOF phenomenon.

After the calibration and the evidence of consistency of the model, the actual dam-break wave flooding has been implemented and simulated.

The Proposed Hydroelectric Dam Baker 2

The so called Baker 2 is a proposed concrete gravitational dam, whose design life is 40 years, that would be located 2 km upstream the confluence of the Rio El Saltòn into the Rio Baker. The project capacity of the station is 360 MW and the average annual power produced would be 2'530 GWh.

The design discharge is 1'275 m^3/s, while the average annual discharge of the Rio Baker is 948 m^3/s. The main design aspects of the dam are described in Table 2.

Dam Baker 2: Concrete gravity type	
Elevation (m)	40
Height (m)	93
Lenght (m)	320
Width (m)	8
Reservoir surface (ha)	3600
Reservoir volume (hm^3)	380

Table 2 – Baker 2: design characterization

The dam Baker 2, according to the EIA published by Hydroaysén, is meant not to have any significant effect on the regulation of flow regime, namely it would cause flow variation not greater than the 5% of the natural daily and monthly variation. The average retention time, for the design discharge, is 8 hours.

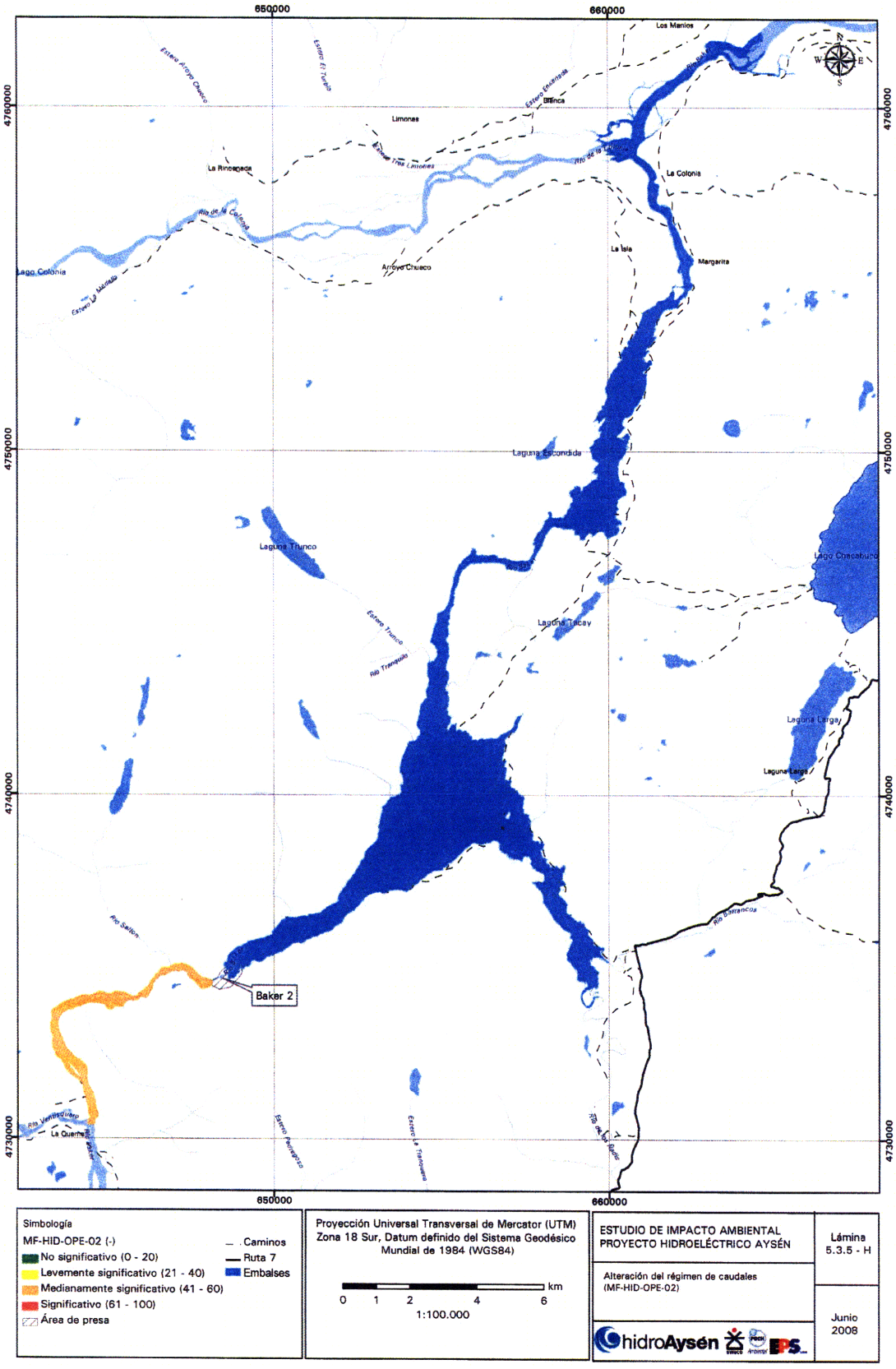

Figure 5 – Baker 2 reservoir (from HydroAysen EIA)

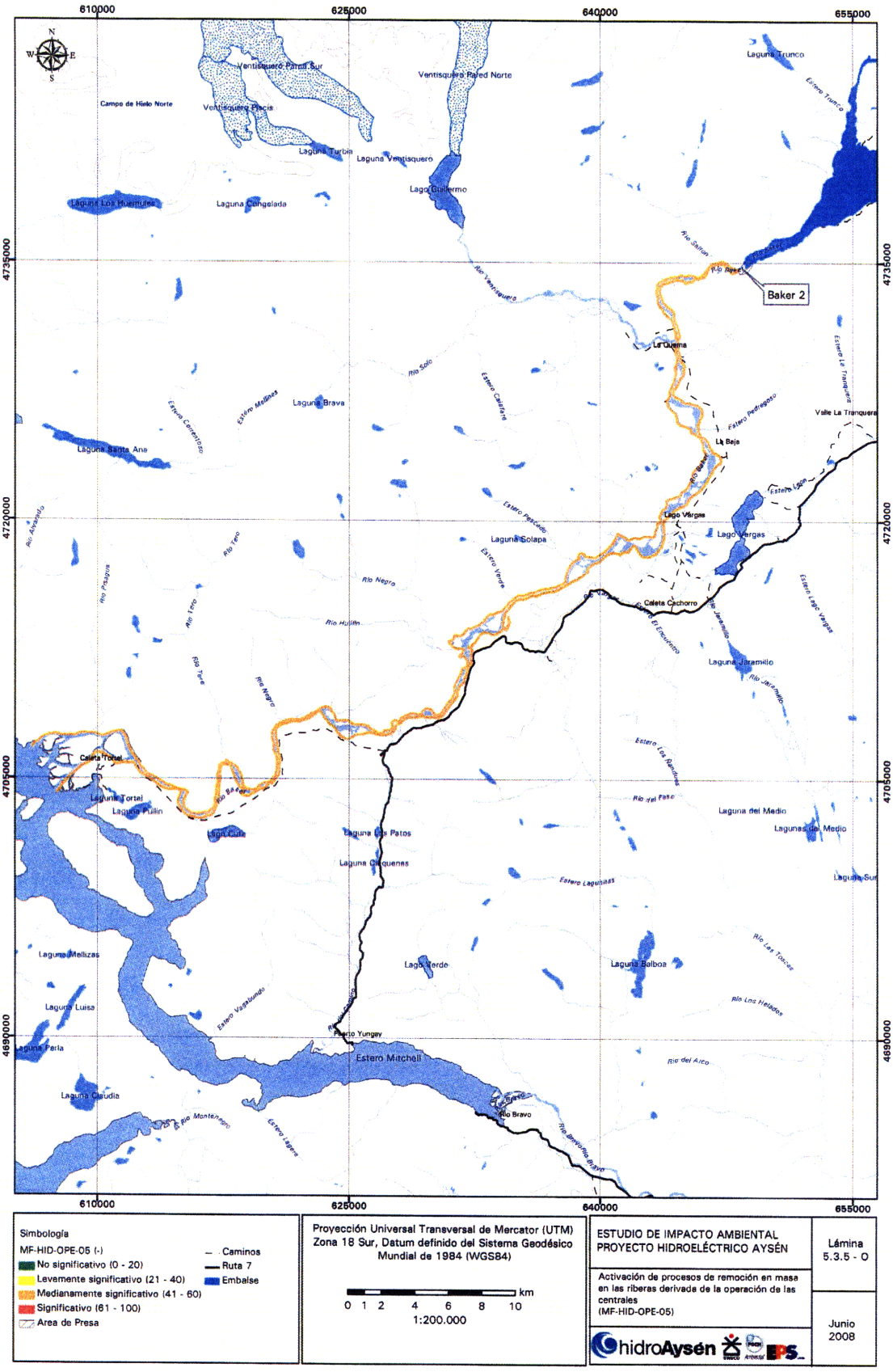

Figure 6 – Rio Baker downstream dam Baker 2 (from HydroAysen EIA)

4.1 Dam Site

On January 2009 an on-site field trip in the Aysén Region has been organized.

During that period the Rio Baker watershed has been analyzed carefully with a complementary raft experience from his origin Bertrand Lake, fed by general Carrera Lake, until his delta into the Pacific Ocean near the town of Caleta Tortel.

The on-site evaluation has allowed appreciating the characteristic of the vegetation surrounding the waterway and the riverbed granulometry in order to define the appropriate values of the Manning coefficient downstream the location of the proposed dam Baker 2.

The site inspection of Caleta Tortel gave thorough information about the context of the major town threatened by the impact of a potential dam break failure.

4.1.1 Topographic Information

Within the process of data collection, the gathering of topographic material has been the most challenging. The principal office of the Dirección General de Aguas (DGA), Chile's state body responsible for promoting the management and administration of water resources, hasn't been able to provide any orthographic, topographic, military or cadastral plan of the valley.

The only available topographic data have been provided freely by the U.S. Geological Survey website.

The Digital Elevation Model (DEM) provided by the USGS is a product of the Shuttle Radar Topography Mission (SRTM) is a joint project between NASA and NGA (National Geospatial-Intelligence Agency) to map the world in three dimensions. SRTM utilized dual Spaceborne Imaging Radar (SIR-C) and dual X-band Synthetic Aperture Radar (X-SAR) configured as a baseline interferometer, acquiring two images at the same time. These images, when combined, can produce a single 3-D image. Flown aboard the NASA Space Shuttle Endeavour February 11-22, 2000, SRTM successfully collected data over 80% of the Earth's land surface, for all area between 60 degrees N and 56 degrees S latitude.

SRTM data were processed from raw radar echoes into digital elevation models at the Jet Propulsion Laboratory (JPL) in Pasadena, CA. These original data files had samples spaced ("posted") at intervals of 1 arc-second of latitude and longitude (about 30 meters at the equator). These data were then edited by the National Geospatial-Intelligence Agency (NGA, formerly the National Imagery and Mapping Agency), and distributed as part of their DTED® product set.

The editing, also referred to as finishing, consisted of delineating and flattening water bodies, better defining coastlines, removing "spikes" and "wells", and filling

small voids. This set is publicly available at two postings: 1 arc-second for the United States and its territories and possessions, and 3 arc-seconds for regions between 60 degrees N and 56 degrees S latitude. (Source: http://seamless.usgs.gov).

4.1.2 Topographic Editing using ArcGIS 9.3

The data downloaded from the USGS website was a 90-meter DEM affected by some issues e.g. occasional bad data on the riverbed and holes in the dataset in certain places.

The DEM has been cleaned and elaborated using ArcMap from ArcGIS 9.3.

The dataset has been imported, reduced to the area of interest, the watershed has been defined carefully, and the occasional holes has been located and eliminated performing a moving average. The dataset provided by the moving average has been merged retaining for the final map the best data available (the first) from each passage of the average.

Dam-Break Modeling

4.2 Calibration

A fundamental process in the dam failure impact assessment is the calibration of the model. The existence of previous flood records allows calibrating the model matching the available flood inundation data to the numerical dam-break model results. This analysis tests the accuracy of the model adopted.

The event simulated to calibrate the model has been the Glacial Lake Outburst Flood recorded on March 5th 2009.

This choice was driven by the fact that the GLOF under consideration is the latest and the one with the biggest peak discharge recorded so far. There are still many concerns about the impact of GLOFs on the safety of the downstream Baker valley, with or without dam, hence this flood simulation is an additional tool for a better understanding of the phenomenon and his potential impact.

4.2.1 Hydrologic Data Collection

The hydrologic data downloaded from the DGA website enabled the definition of the flow hydrograph associated to the GLOF event analyzed.

A detailed description of the GLOF impact simulation will be treated in Chapter 5. Nevertheless, in order to give consistency to the next paragraphs, it is anticipated that the results of the calibration process guaranteed the model accuracy desired.

4.3 *Dam-Breach Analysis*

The most important component of a dam-break analysis is the definition of reasonable breach parameters, which are highly difficult to be accurately predicted.

The breach width and breach time have a great influence on the forecast of the outflow and the flooded area downstream the dam. The developing time for a breach is defined as the point where dam failure is imminent and end when the breach has reached its maximum size. For relatively small reservoirs, the dam-break peak outflow usually occurs before the breach is completely developed, resulting from a consistent drop in reservoir levels during the formation of the rupture, while in large reservoirs the peak outflow occurs as soon as the breach has extended to its maximum size.

Breach parameters and related dam-break peak outflow have been defined, using the limited available data, adopting two methods:

- The NWS SMPDBK model developed by the National Weather Service (NWS)
- The Generalized Ritter Dam-Break Solution (1892) suggested by the USACE

4.3.1 NWS Simplified Dam-break model

The empirical predictor equations used by the NWS SMPDBK model are based on regression analyses of a number of historical breaks, and they have been ultimately described by Froehlich in 1995.

NWS SMPDBK Peak discharge:

$$Q_p = 3.1b\left\{\frac{C}{T+\frac{C}{\sqrt{H_d}}}\right\}^3 \qquad \text{where:} \qquad C = \frac{23.4S_a}{b} \quad \text{and}$$

Q_p = Peak flow (cfs)

S_a = Surface Area (Ac)

H_d = Breach Head (ft) - defined as Depth of Water at time of Breaching

b = Breach width (ft)

T = Time (Minutes)

NWS SMPDBK concrete gravity dam Breach:

$$b = 5\,H_d$$

where:

b = Breach width (ft)

H_d = Breach Head (ft) - defined as Depth of Water at time of Breaching

The estimated breach width resulting from the model, given the available data, is b = **265** m.

The corresponding peak outflow is Q_p = **61'098** m^3/s.

4.3.2 Generalized Ritter Dam-Break Solution

For completeness and to provide an alternative flood forecast, the peak discharge has been calculated also according to the USACE *Guidelines for Calculating and routing a Dam-*

Break Flood.

Peak discharge:

$$Q_p = \frac{8}{27} b \sqrt{g} H_d^{3/2}$$

where:

Q_p = Peak flow (m^3/s)

H_d = Breach Head (m) - defined as Depth of Water at time of Breaching

b = Breach width (m)

g = gravity coefficient (m/s^2)

The standard guidelines recommend to consider a standard dam breach corresponding to the 30% of the total dam length:

$$b = 0.3\,L$$

where:

b = Breach width (m)

L= Dam length (m)

The estimated breach width resulting from the model, given the available data, is b = **96** m.

The corresponding peak outflow is Q_p = **34'375** m^3/s.

4.3.3 Estimated Peak Discharge at Dam Site

In order to guarantee a cautious analysis, the final decision disposed to chose for the most conservative estimation of the peak flow, that is the Q_P estimated through the NWS SMPDBK model.

The breach time has been therefore evaluated using the relations adopted by the NWS SMPBDBK model for a concrete gravity dam:

$$t_b = \frac{H_d}{40}$$

where:

t_b = Breach Time (minutes)

H_d =Breach Head (ft) - defined as Depth of Water at time of Breaching

The estimated breach width resulting from the model is **7.6** minutes.

5. Dam-Break Simulation

ORSA Code

ORSA Code is a 1-Dimensional computational model which simulates flood wave propagation and identifies flood prone areas as the areas where the ground is lower than the computed water elevation. The software has been developed by a research collaboration between the University of Pavia [3] and the University of Rome, La Sapienza [4].

The hydraulic simulation reproduces different scenarios mapping the resultant flooded areas on the digital elevation model (DEM) of the surface topography.

5.1 Numerical Solvers

ORSA Code adopts two different finite volumes solvers to integrate the Shallow Water Equations, the simplified 1-D governing equations of unsteady open channel flow: the Roe scheme and a modified Lax - Friedrichs scheme.

As will be discussed in Chapter 6, those mathematical models solve the SWE written in conservative form, which allows the software to reproduce the discontinuities of a flow regime variations without incur in instabilities of the solution.

The shock-capturing capability of the software when dealing with transcritical flow regime, which is mainly due to sudden changes in the channel geometry, has practical interest.

5.2 Surface Topography Acquisition and Analysis

The Rio Baker Digital Elevation Model (DEM), already processed in a previous passage (see §4.1), has been uploaded and verified. *ORSA Code* interface allows to automatically outlining the contour lines for a given distance. The contour lines have been defined every 20 meters.

5.2.1 Breakline

The breakline is a poliline that has been drawn into the riverbed in order to define the axis line of the channel. The breakline starts at the location of the proposed dam Baker 2 and has been traced until the Rio Baker delta; its total length is 65 km.

---

[3] L. Natale, G. Petaccia , M. Zanotti

[4] F. Savi

5.2.2 Sections

The definition of the cross sections is an accurate passage of the topography editing. The output values of the calculation are always referred to a particular section. Hence, for a thorough understanding of the flooded area in a certain location, for instance Caleta Tortel, an attentive choice is very important. The cross sections are always perpendicular to the breakline. 66 sections have been edited.

5.2.3 Visualization

Although the correlation between *ORSA Code* topographic interface and another topographic tool is optional, it resulted of great importance in understanding the planimetry and in confirming the coherency of the information.

Some interesting comparison between *ORSA Code* interface and *Google Earth* images are shown in figures here below. Figure 7

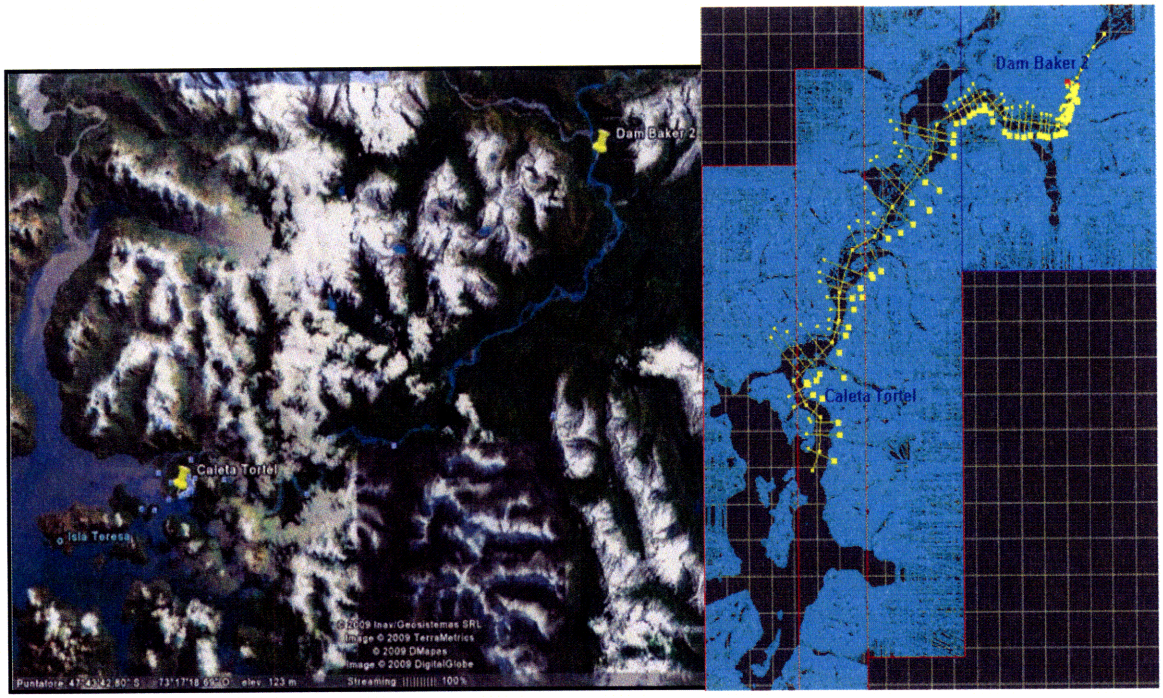

Figure 7 – Rio Baker downstream Baker 2 dam. View from Google Earth and ORSA Code interface

5.2.4 Assignation of Manning's Coefficient

Manning's roughness coefficient values are used in the Manning's formula for flow calculation in open flow channels. Roughness coefficients represent the resistance to flood flows in channels and flood plains.

Roughness coefficient should be varied to account for seasonal variability. Floods often occur during the winter when there is less vegetation, while in spring vegetation growth is denser. Nevertheless, the calibration case study, as said, has

been a simulation of a GLOF, phenomenon always happening during warm season (Spring/Summer) when ice melting occurs. For this reason the Manning's coefficient choice refers to the spring vegetation growth.

For a more accurate dam-break analysis, the values of the Manning roughness coefficient should be varied in each cross-section according to the local survey. When local analyses are not accurate enough, only one roughness coefficient might be sufficient in representing the whole floodplain.

On account of these considerations, the Manning's roughness coefficient assigned has been **0.03625 (**
Table 3).

Surface Material	Manning's Roughness Coefficient -n-
Earth channel - gravelly	0.025
Earth channel - stony, cobbles	0.035
Floodplains - pasture, farmland	0.035
Floodplains - light brush	0.05
Average value	**0.03625**

Table 3 – Manning's Roughness Coefficient values

GLOF Simulation

The simulation of the Glacial Lake Outburst Flood of March 5th 2009, and the related flooded area have been a fundamental process for the model calibration. (see §4.2)

The next paragraphs contain the assumption and the characterizations which resulted more suitable for a fair matching of the available flood inundation data to the numerical model outputs.

5.3 Initial Conditions

ORSA Code interface is able to simulate the wave propagation during a flood, specifying a certain section and its water level, or a situation of "sunny day", assuming dry bed.

The appropriate choice has been the assumption of the condition dry bed (or "sunny day").

5.4 *Boundary Conditions*

The definition of the Boundary Conditions, that is the assignation in a certain section of a known value from which proceed in the calculus of the unknowns, is a critical passage of the analysis and it is always affected by a certain degree of incertitude. The manipulation of the B.C., evaluating their different impacts on the evolution of final results, is an important goal of the calibration process.

Hereinafter follows a description of the B.C. finally assigned to the GLOF case study.

5.4.1 Upstream B.C.

Considering a supercritical flow, two conditions have been assigned in the initial upstream section:

- Fr = 1, where the critical value of the Froude number [5] indicates that the initial section is a *control section*
- GLOF hydrograph (represented in Figure 8), based on the hydrologic data downloaded from the DGA website.

[5] The Froude number, Fr, is a dimensionless value that describes different flow regimes of open channel flow. The Froude number is a ratio of inertial and gravitational forces.

$Fr = \frac{v}{\sqrt{hg}}$ where:

v is the flow velocity
g is the gravitational acceleration
h is the hydraulic depth

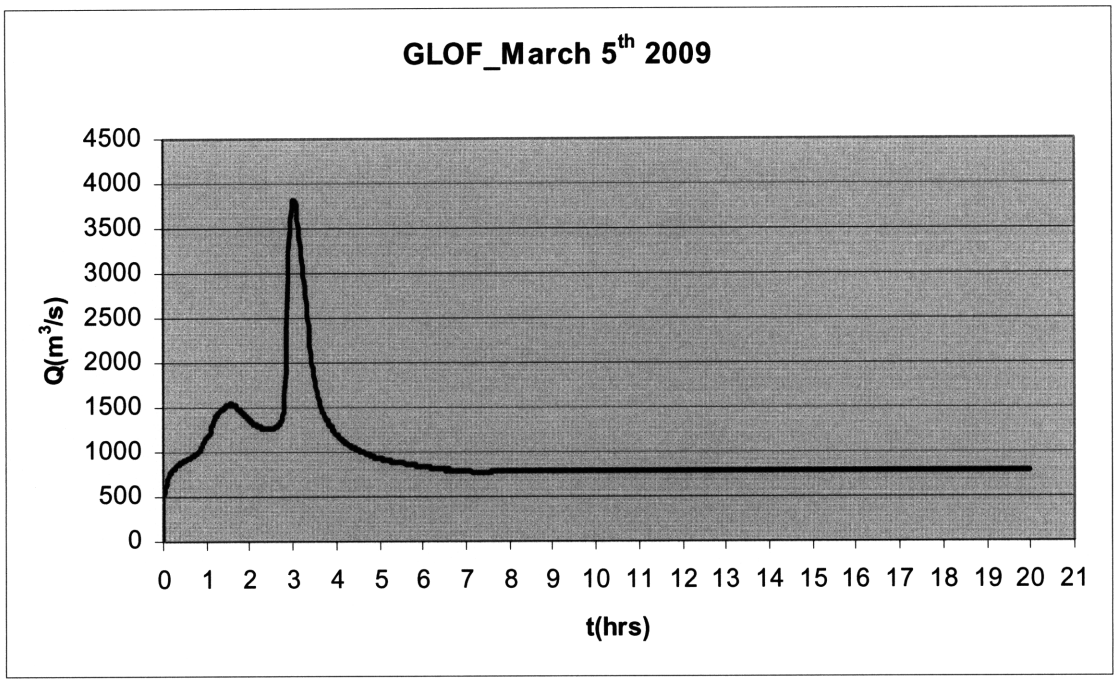

Figure 8 – Hydrograph of the GLOF event that happened on March 5th 2009

The total duration of the flood wave have been chosen to be 20 hours, after some attempts and an evaluation of the average flow velocity, in order to guarantee the reaching of the closure section (the simulation stops as soon as the wave is completely released from the initial section).

5.4.2 Downstream B.C.

- Fr = 1

Assigning a state of critical flow has two different implications depending on the flow wave state arriving at the section. If case the wave is supercritical, this B.C. is redundant. In case the wave is subcritical, this B.C represents the closure of the numerical simulation. The last case is the more likely, because it represents a wave jumping into the ocean, where the actual water depth is below critical depth.

5.5 Simulation Characterization

- CFL = 0.1 [6], the solution stability has been guaranteed
- *Dt* = 0.1 s, where *Dt* is the minimal integration time-step

[6]The *Courant–Friedrichs–Lewy condition (CFL)* is a condition for convergence while solving the hyperbolic partial differential equations with time explicit schemes. The time-step must be smaller than a certain time interval in order to have stability in the results.
CFL varies between 0.1 and 1.

5.6 *Results*

The maximum flood experienced in the Baker Valley due to a GLOF can be depicted by a graph on which maximum flooded widths calculated by the software ORSA Code are plotted against drainage area.

This way of representing the simulation results provides the most concise description of the catchment size magnitude.

The results are consistent with the available flood inundation data (*DGA report*, March 6, 2009). The model is therefore calibrated.

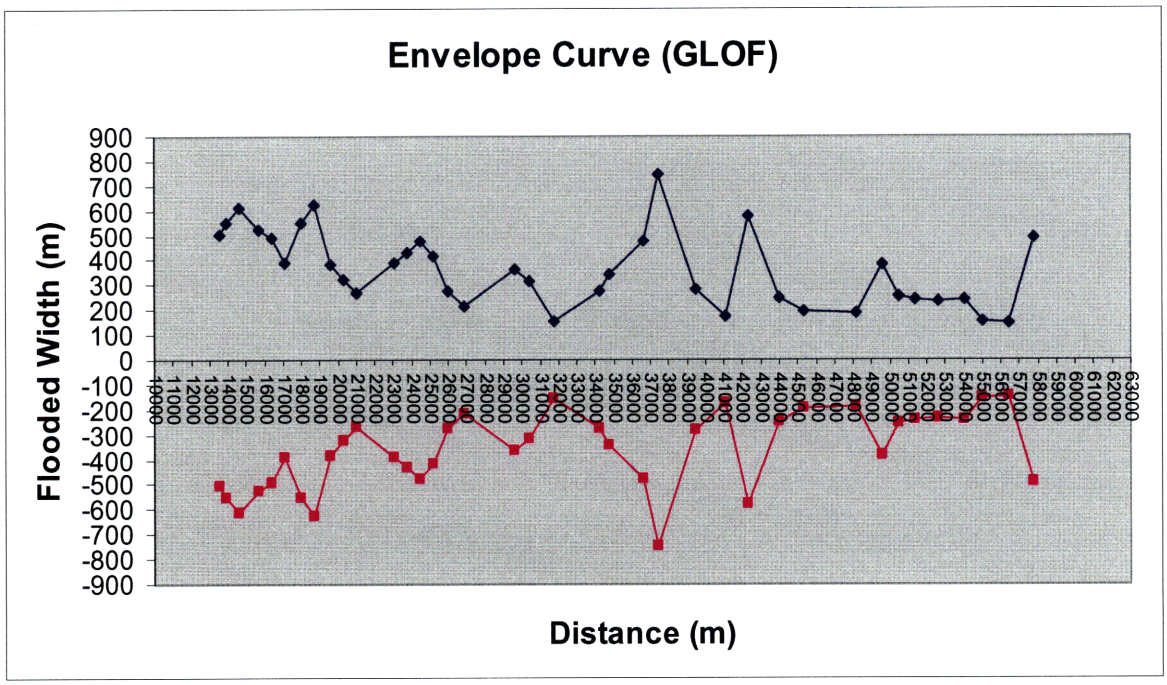

Figure 9 – GLOF flooded width envelope curve

Dam-Break Simulation

The simulation of the Glacial Lake Outburst Flood of March 5th 2009, and the related flooded area have been a fundamental process for the model calibration (see §4.2).

The next paragraphs contain the assumption and the characterizations which resulted more suitable for a fair matching of the available flood inundation data to the numerical model outputs.

5.7 *Initial Conditions*

ORSA Code modeling tools, as illustrated in previous paragraphs, can simulate different scenarios and the resulting downstream inundation map. Due to the spare

availability of hydrologic data, the analysis considers a "sunny day" scenario, which accounts for non-rainfall causes of failure.

The scenario assumes that the breach will occur under normal operating conditions, i.e. there is no added inflow to the reservoir to increase the pool normal full storage.

5.8 Boundary Conditions

5.8.1 Upstream B.C.

Considering a supercritical flow, two conditions have been assigned in the initial upstream section:

- Fr = 1, where the critical value of the Froude number indicates that the initial section is a *control section* (Dam-Breach happens)
- Hydrograph for dam-break wave(represented in Figure 10)

The design hydrograph has been estimated using a two-parameter gamma distribution, commonly used to estimate quantiles of hydrological random quantities.

The gamma distribution is very flexible in fitting data. Its parameters have been gauged in order to fulfill the following requirement:

- peak outflow Q_p = **61'098** m³/s (defined through the NWS SMPDBK model (see §4.3.1)
- breach time t_b = **7.6** min ((defined through the NWS SMPDBK model (see §4.3.1)
- area under the curve **3600** ha (Baker 2 design characterization)

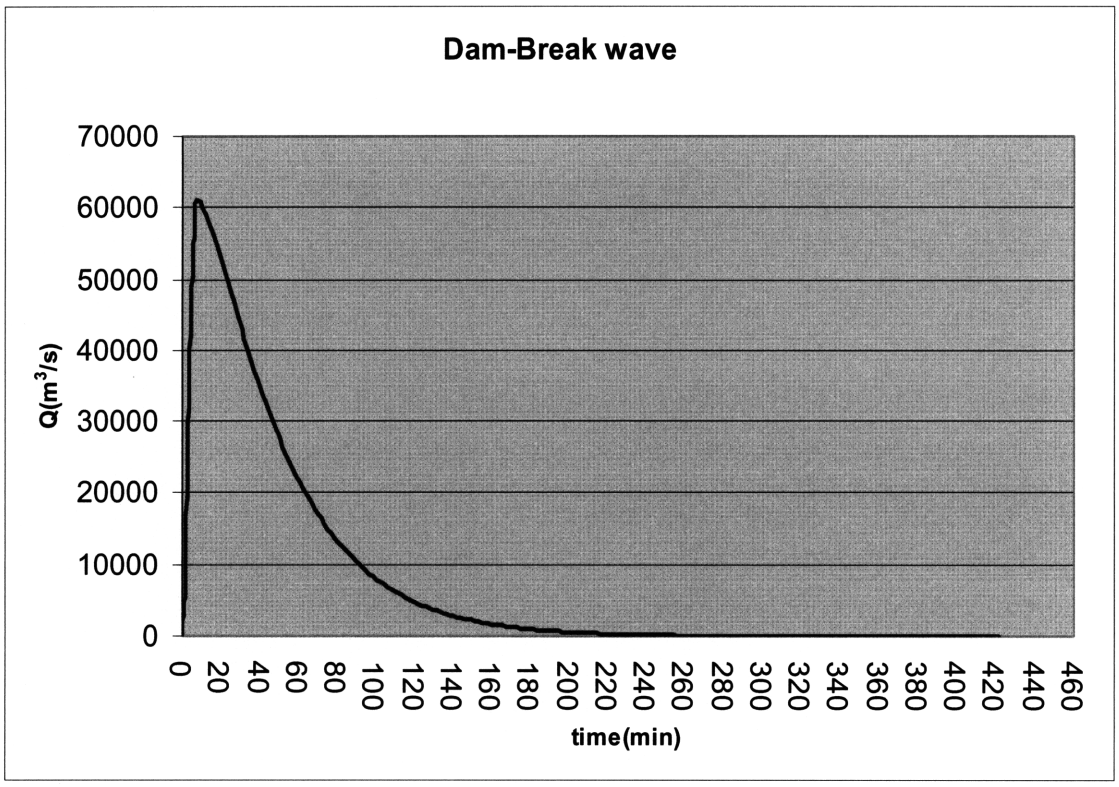

Figure 10 – Dam-break wave hydrograph

5.8.2 Downstream B.C.

- Fr = 1

Assigning a state of critical flow has two different implications depending on the flow wave state arriving at the section. If case the wave is supercritical, this B.C. is redundant. In case the wave is subcritical, this B.C represents the closure of the numerical simulation. The last case is the more likely, because it represents a wave jumping into the ocean, where the actual water depth is below critical depth.

5.9 Simulation Characterization

- CFL = 0.01, the solution stability has been guarantee
- *Dt* = 0.1, where *Dt* is the minimal integration time-step

5.10 Results

5.10.1 Dam-Break Wave Outflow

The following charts represent the dam-break wave discharge downstream Baker 2 dam along the waterway. Each graph corresponds to the indicated time.

For a better understanding of the results, the graphs have been compared in different charts.

Figure 11 shows how the discharge decreases rapidly in time.

After 2 hours from the beginning of the dam-break wave the discharges are too small to be compared with the starting outflow, for this reason they are presented in different charts. Figure 12, Figure 13 and Figure 14 show the final development of the outflows.

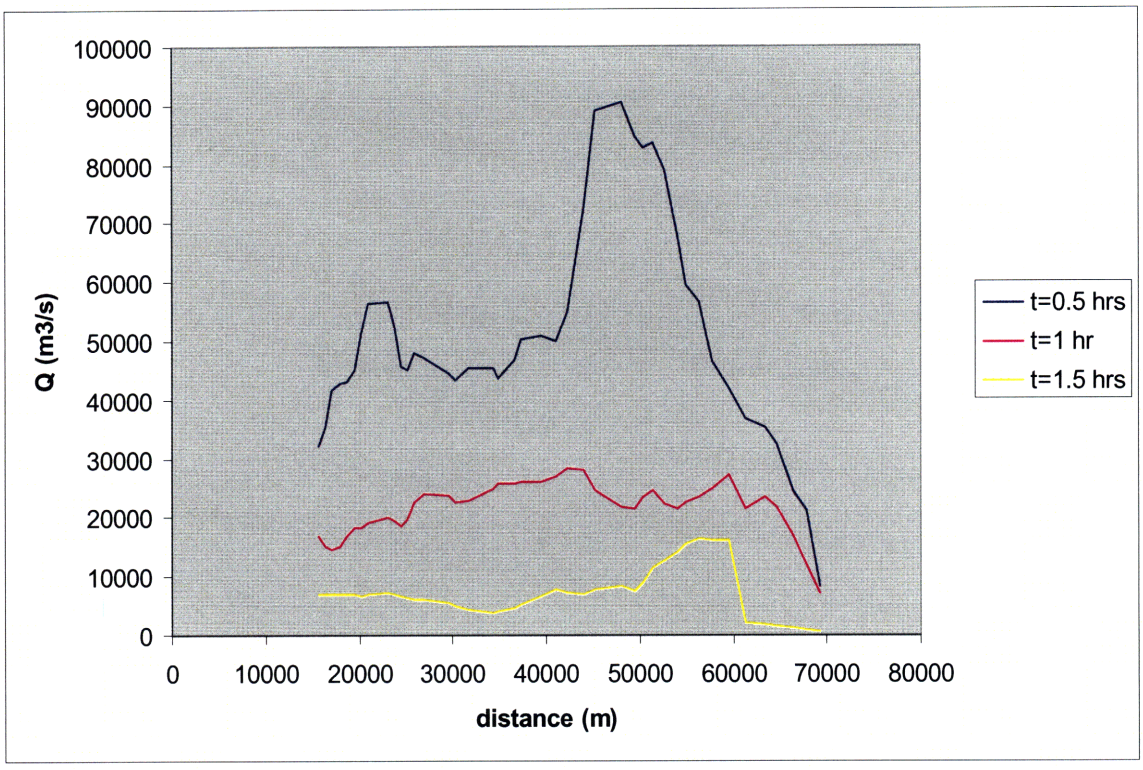

Figure 11 – Dam-break discharge after 0.5 hours, 1 hour and 1.5 hours

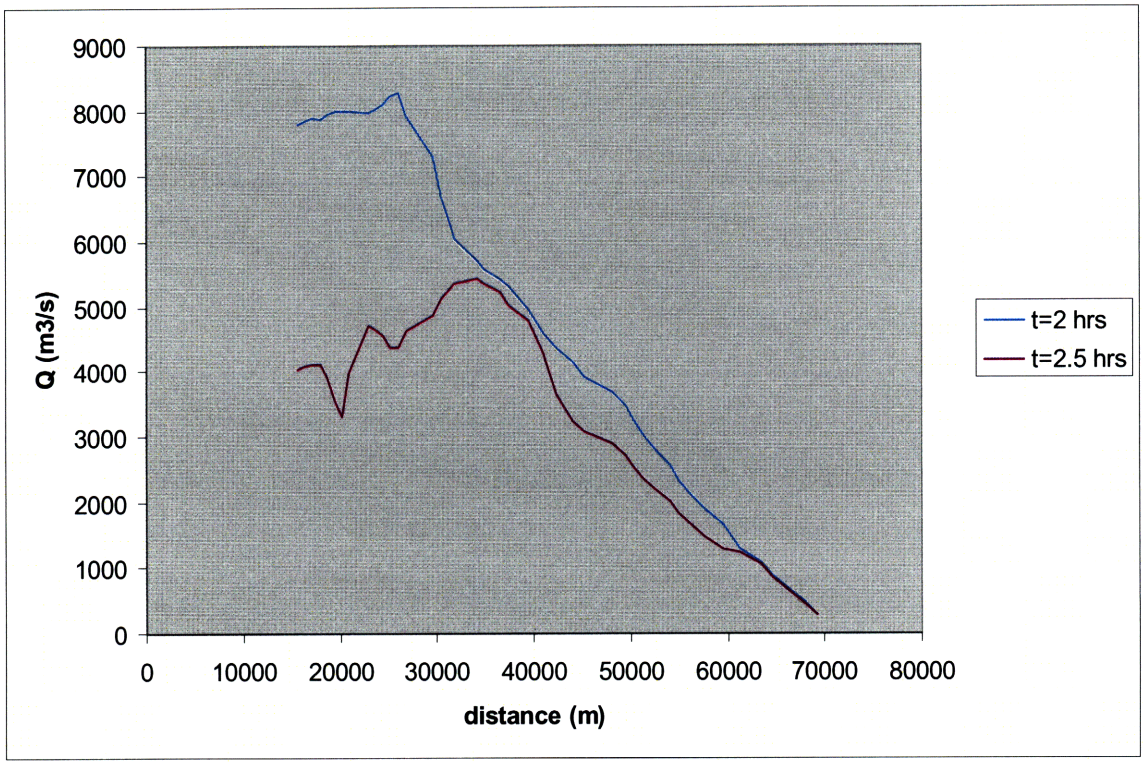

Figure 12 - Dam-break discharge after 2 and 2.5 hours

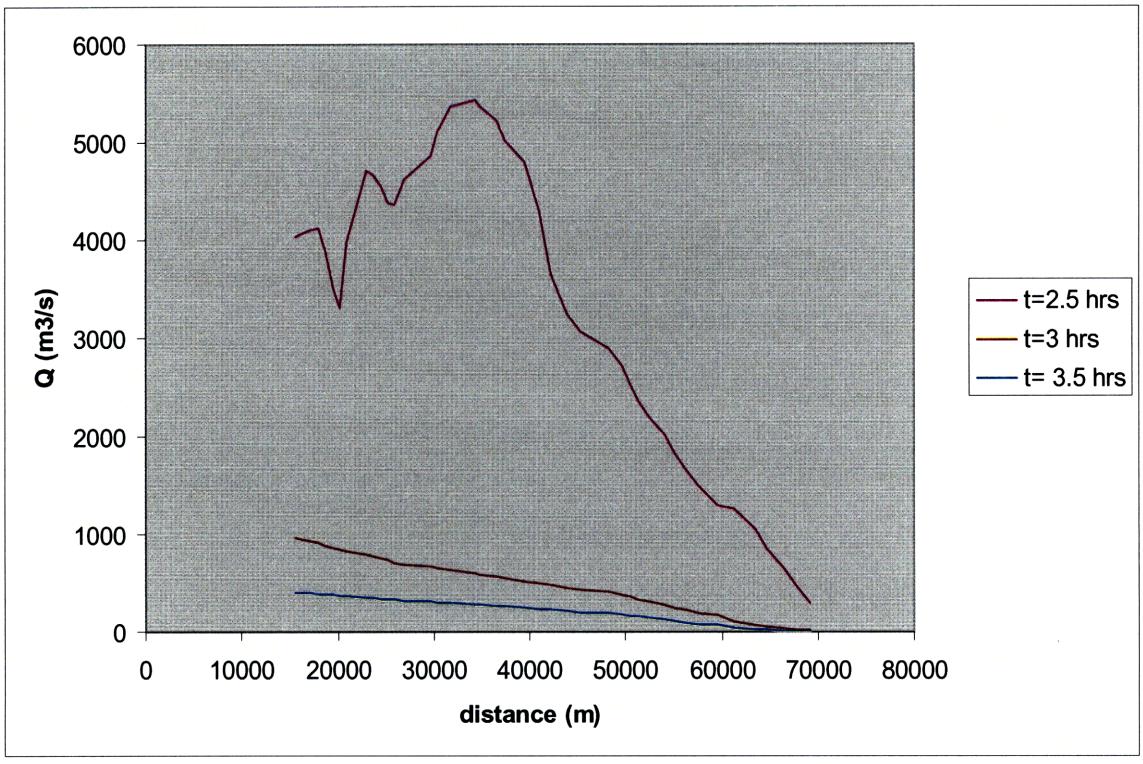

Figure 13 - Dam-break discharge after 2.5, 3 and 3.5 hours

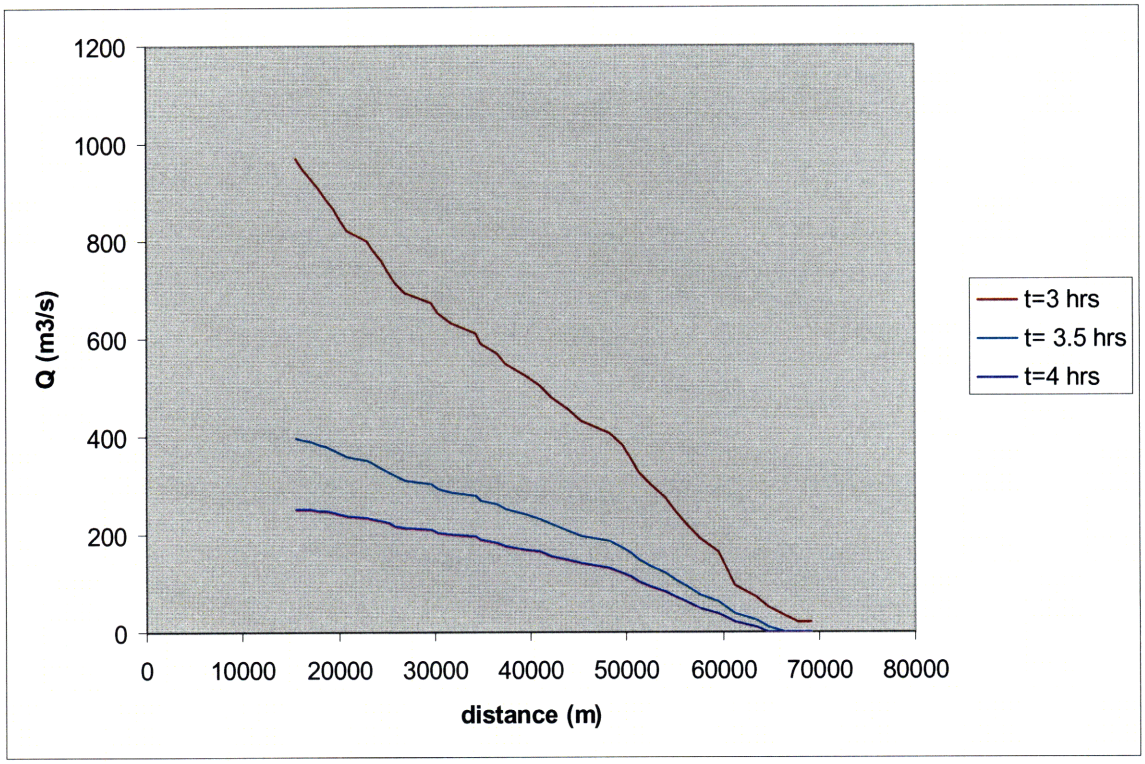

Figure 14 - Dam-break discharge after 3, 3.5 and 4 hours

5.10.2 Water Level

The following chart shows how the water heights develop along different sections at different times. Figure 15

The higher water level presented at the final sections of the progressive are consistent with the physical reality of the case: the final sections correspond to the river delta, where the valley widens: the river flow velocity decreases and consequently the water level increases.

After 3 hours the impact of the dam-break wave on the last sections of the Baker Valley is no more significant.

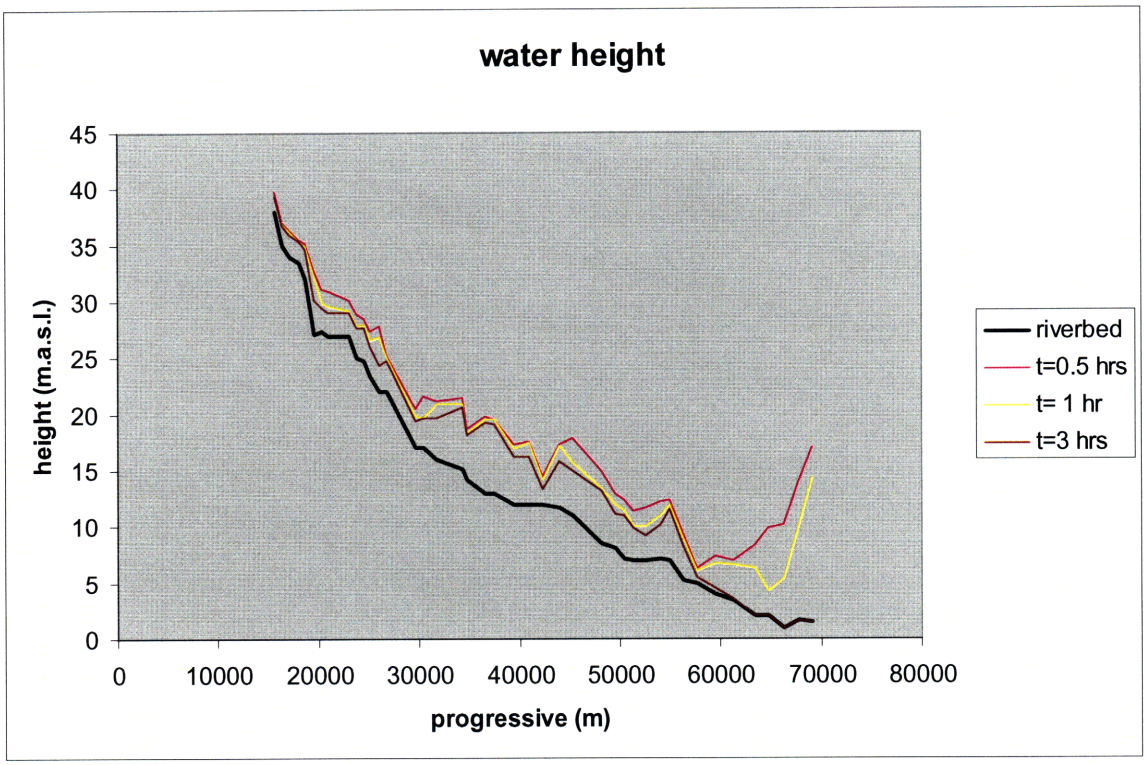

Figure 15 – Water levels at 0.5, 1 and 1.5 hours

5.10.3 Flooded Width

The graph presented hereinafter (Figure 16) shows the flood propagation and the flood routing. The "envelope curve" is obtained by plotting the largest flood peaks versus the drainage area and represents the maximum flooded width in each section evaluated in all the time intervals.

The change in shape of the flooded area corresponds to the change in shape of the valley, which narrows and enlarges successively many times from the Baker 2 dam to the river delta.

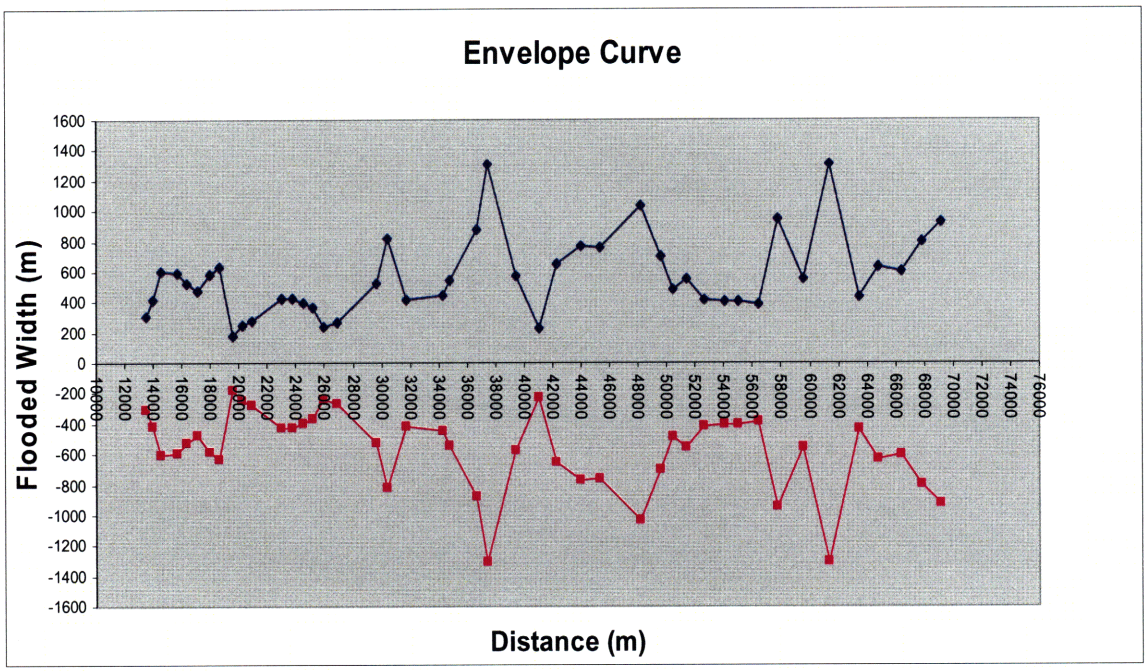

Figure 16 – Flooded width envelope curve

5.10.4 ORSA Code Output

ORSA Code presents a flood simulation tool which allows the user to visualize the flood propagation in real time. An image of the resulting flooded area is given in Figure 17.

The first red line corresponds to the Baker 2 dam proposed location, while the yellow lines correspond to each design section.

Figure 18 is focused on the river delta, which coincides with the location of Caleta Tortel, the main village of the area. With 320 inhabitants (Census, 2002), Caleta Tortel consists mainly of stilt houses built along the coast for several kilometres. Instead of conventional streets there are wooden walkways.

The results of the dam break-analysis show a high-risk level for the population living in the aforementioned area.

This simplified assessment is not accurate enough to adequately calculate the population at risk. A more comprehensive assessment of the failure impact zone requires details about the local distribution of the population, the location, the number, the elevation of each building and the definition of the most critical zones (e.g. hospitals, school).

ORSA Code is able to define accurately the flooded area, nonetheless a planimetric background is necessary to interpret the actual risk for the downstream population and accomplish a thorough dam-break impact assessment.

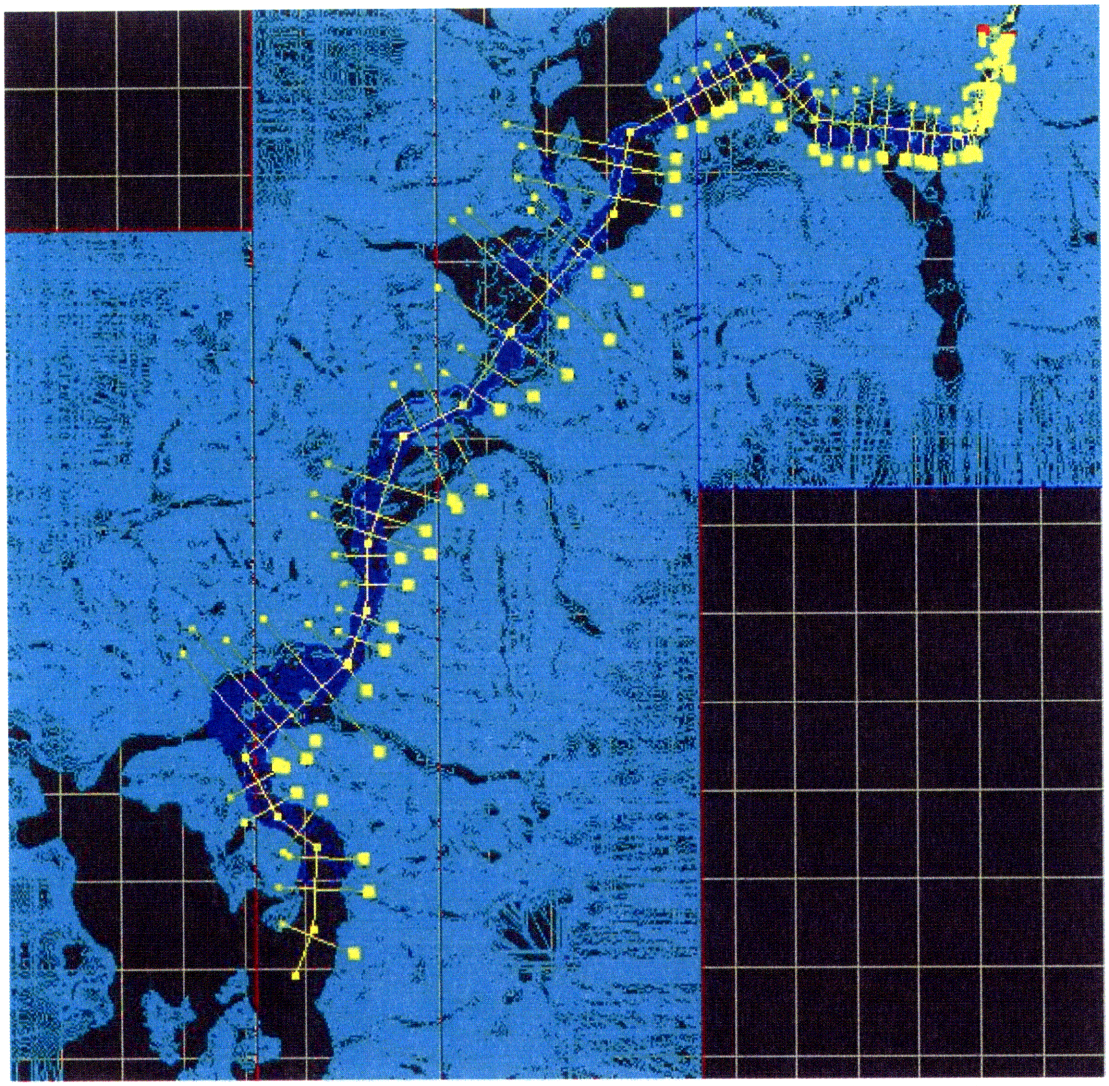

Figure 17 – ORSA Code, overview of flood propagation

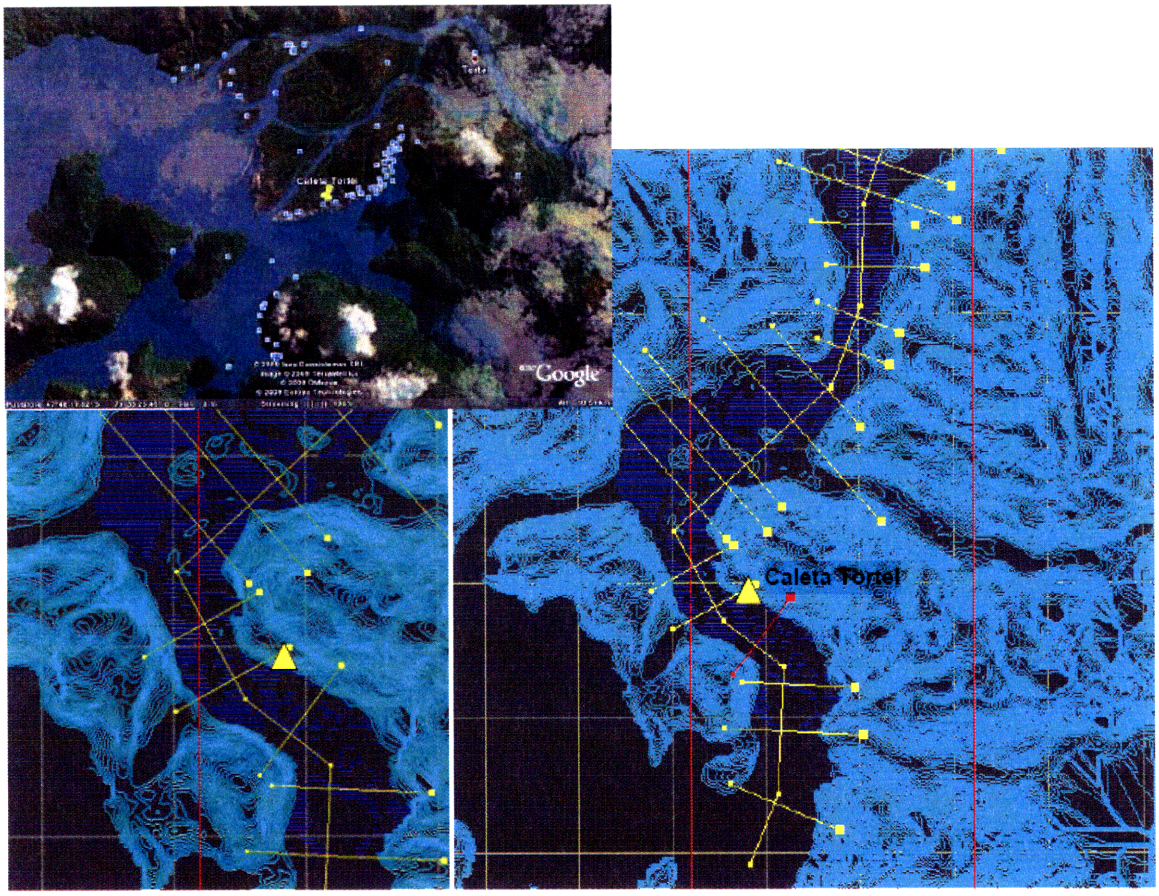

Figure 18 – ORSA Code, flood propagation at the Rio Baker mouth and image of the area downloaded from Google Earth

6. Literature Review: Dam-Break Modeling

In dam safety programs and flood forecast, dam-break modelling is an indispensable tool to evaluate dam induced risk and to support emergency plan, optimizing response efforts and directing first-response teams to damaged areas.

However, a better understanding of flood predictability and model efficiency is needed before such systems can be effectively implemented.

This section presents and compares some one-dimensional numerical models and their basic mathematical and numerical expressions.

Hydrodynamic Model: Shallow Water Equations

Despite the three-dimensional structure of the detailed free surface flows, it is possible to simplify the governing equations of unsteady open channel flow in cases in which the longitudinal flow scale is greater than the transversal dimensions and the problem is approximated as variable only in the spatial direction along the main flow (Pérez et al. 2006). (Figure 19).

The conservation of mass and momentum along the direction of the main flow is governed by the shallow water or Saint-Venant equations, derived from Navier-Stokes equations by making certain assumptions.

This is a reasonable approach in many practical applications assuming that water is incompressible, pressures are hydrostatic, vertical accelerations are negligible, and waves are nondispersive. The Saint-Venant equations are a nonlinear hyperbolic system mathematically analogous to the compressible Euler equations.

Under the De Saint-Venant hypothesis, the conservation laws are (Cunge et al. 1980)

$$\frac{\partial U}{\partial t}+\frac{\partial F}{\partial x}=R$$

With

$$U=(A,Q)^T,$$

$$F=\left(Q,\frac{Q^2}{A}+gI_1\right)^T,$$

$$R = \left(0, gI_2 + gA(S_0 - S_f)\right)^T$$

A is the wetted cross-sectional area, Q, the discharge and g, the acceleration due to gravity. I_1 represents a hydrostatic pressure force term as described in Cunge et al. (1980).

I_2 accounts for the pressure force in a volume of constant depth h due to longitudinal width variations.

S_0 is the bed slope; S_f stands for the energy grade line.

Garcia-Navarro et al. (1999) define it in terms of the Manning's roughness coefficient n as:

$$S_f = \frac{Q|Q|n^2}{A^2 R^{4/3}},$$

The hydraulic radius is R = A/P, P being the wetted perimeter.

The Jacobian matrix of the system is

$$A = \frac{\partial F}{\partial U} = \begin{pmatrix} 0 & 1 \\ c^2 - u^2 & 2u \end{pmatrix},$$

Where u = Q/A and $c = \sqrt{gA/b}$. According to the formulation of Garcia-Navarro et al. (1999), the eigenvalues and eigenvectors of A respectively are:

$$a^{1,2} = u \pm c$$

$$e^{1,2} = (1, u \pm c)^T.$$

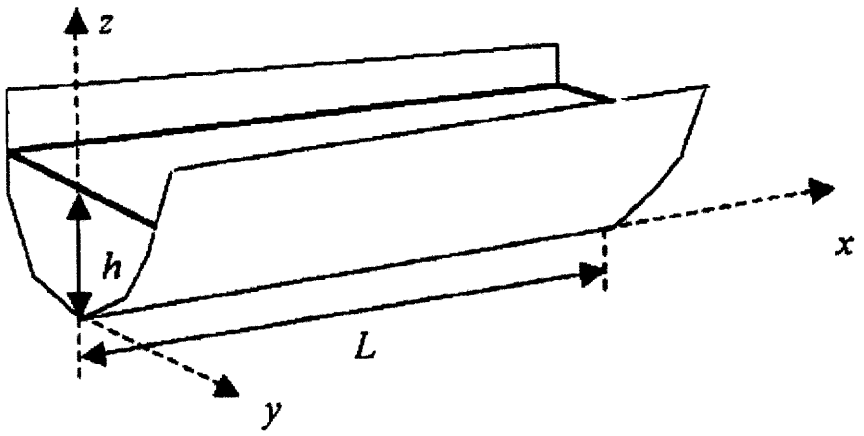

Figure 19. One-dimensional flow along x direction. (Pérez et al. 2006).

6.1 Numerical Solvers

The first difficulty in any case of integration of a system of quasi-linear partial differential equations is the choice of the numerical scheme.

The numerical modelling of unsteady flow in rivers is a complicated task and the difficulties grow as the pretensions to obtain better quality or more general solutions do (Cunge et al., 1980).

Currently there is a wide range of techniques suitable for numerical integration of shallow water flow equations (SWE). However, it has traditionally been difficult to have a single method able to reproduce automatically any general situation.

Hereafter 4 schemes are described. They are all explicit in time.

Scheme 1. is usually adopted for subcritical flows because it presents instabilities during flow regime transitions (passage through critical phase) or supercritical flows; Scheme 2. is applicable also for flows with a few flow regime transitions; Schemes 3. and 4. are general for subcritical and supercritical flow.

Schemes 1., 2., and 3. are finite difference (FD) while Scheme 4. and 5. are finite volume (FV).

6.1.1 Lax-Friedrich's Scheme

The Lax-Friedrichs (LxF) method is a basic method for the solution of hyperbolic partial differential equations (PDEs). Its use is limited because its order is only one, but it is easy to implement, applicable to general PDEs, and has good qualitative properties because it is monotone and very robust. The LxF method is often used to show the effects of dissipation, but it is not actually a dissipative method (Strikwerda 1989).

For the general case of homogeneous conservation system

$$\frac{\partial U}{\partial t}+\frac{\partial F}{\partial x}=0$$

the procedure of nodal updating of a regular grid for each time step Δt is:

$$U_i^{n+1}=\theta U_i^n+\frac{1-\theta}{2}\left(U_{i+1}^n+U_{i-1}^n\right)-\frac{\Delta t}{2\Delta x}\left(F_{i+1}^n-F_{i-1}^n\right)$$

$0 \le \theta < 1$.

The usual value adopted for θ is 0.1.

6.1.2 MacCormack's Scheme

In computational fluid dynamics, the MacCormack method is a second-order finite difference discretization scheme widely used for the numerical solution of hyperbolic partial differential equations (hyperbolic PDEs).

It is a technique of proved efficiency for unsteady open channel flow modelling (Garcia-Navarro and Saviron, 1992; Garcia Navarro and Zorraquino, 1993; etc).

It is second-order accurate in both space and time: it offers good resolution and it is conceptually very simple.

It is composed of a sequence of two sub-steps in which the spatial derivatives are taken in alternate directions.

Considering the general case of homogeneous conservation system

$$\frac{\partial U}{\partial t}+\frac{\partial F}{\partial x}=0$$

it proceeds as follows:

Predictor step (with a "provisional" value of u at time n+1)

$$U_i^p=U_i^n-\frac{\Delta t}{\Delta x}\left(F_{i+1}^n-F_i^n\right)$$

Corrector step

$$U_i^c = U_i^p - \frac{\Delta t}{\Delta x}\left(F_i^p - F_{i-1}^p\right)$$

The final solution is given by

$$U_i^{n+1} = \frac{1}{2}\left(U_i^p + U_i^c\right).$$

6.1.3 TVD Methods

With the total variation diminishing (TVD) method, some classical numerical schemes are reformulated improving their performance without great effort.

Only monotonicity preserving schemes, which never provide non-physical solutions, are TVD. Godunov's theorem proves that only first order linear schemes are monotone and are therefore TVD.

Garcia-Navarro et al. (1999), propose a reformulation of the MacCormack method adding a conservative and non-linear modification of the scheme to make it non-oscillatory at local extrema without losing its accuracy in other regions of the flow.

A first order (Lax–Friedrich's), a second order (MacCormack) and a high resolution (TVD MacCormack) explicit finite difference schemes are applied to the simulation of 1D unsteady flow in rivers (Garcia-Navarro et al. 1999).

While for smoother situation the three methods perform well, the presence of extreme slopes and strong changes in the irregular geometry represent a source of numerical errors.

In these kinds of problem, the TVD version of the MacCormack scheme has a clear superiority, overall in mass conservation ability. (Figure 20).

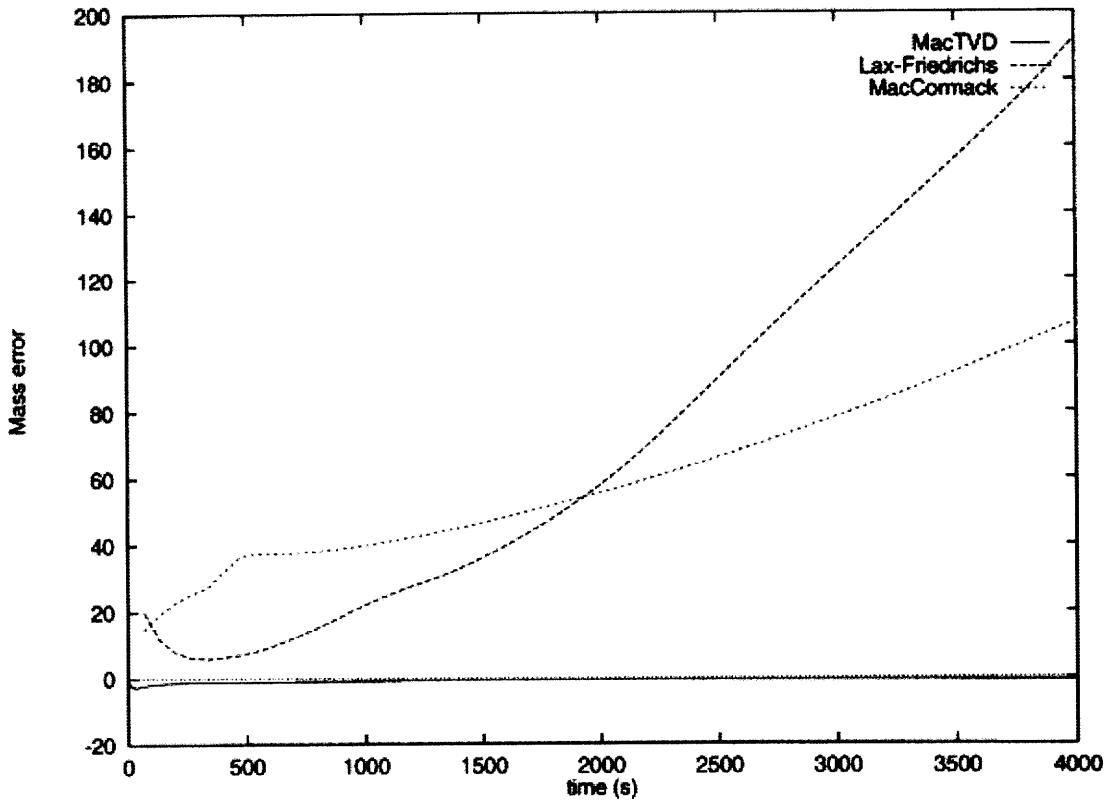

Figure 20- Improvement provided by the TVD scheme. (Garcia-Navarro et al. 1999).

6.1.4 Roe's Method

It's a strategy for obtaining numerical solutions to hyperbolic initial-value problems. (Roe, 1981).

The Roe's approximate Riemann solver applied to an upwind finite volume method has proved efficient for unsteady shallow water problems over a fixed bed both in simple cases and in cases involving variable bed slope and channel width (García-Navarro and

Vázquez-Cendón 1999), its accuracy and stability constraints having been studied in Burguete and Garcia-Navarro (2001).

The method is based on the local linearization achieved by means of an approximated

Jacobian matrix $\widetilde{J}$, such that

$$\partial F = \widetilde{J}\partial U$$

with $\partial U = U_{i+1} - U_i$ and built according to a series of necessary conditions for conservation and consistency (Hubbard and García-Navarro 2000).

The first order explicit Roe's method is suitable for the description of rigid landslide movements and their interaction with shallow water bodies. (Perez et al 2006).

6.1.5 Lax-Friedrich Type Scheme applied on a staggered grid

This is a semi-implicit I order scheme applied on a staggered grid; the momentum equation is written according to the characteristics of the flow in the current node. This scheme, developed by Natale and Savi (1992) modifying the scheme proposed by Sielecky (Vreugdenhil 1989), is intuitive from the physical point of view and easy to implement. The momentum equation is fully explicit and reads:

$$Q_{i+1/2}^{n+1} = Q_{i+1/2}^{n} - \Delta t \cdot M_{i+1/2} - \frac{\Delta t}{\Delta x_{i+1/2}}\left(gI_{i+1} - gI_{i-1}\right) + \Delta t \cdot S_{i+1/2}$$

where

$$M_{i+1/2} = \frac{1}{\Delta x_{i+1/2+s}} \cdot \left(\frac{Q^2}{\hat{A}}\bigg|_{i+1/2+s}^{n} - \frac{Q^2}{\hat{A}}\bigg|_{i-1/2}^{n} \right)$$

$$s = \begin{cases} 0 \; if & F_{i+1/2}^{n} \geq 1 \\ 1 \; if & F_{i+1/2}^{n} < 1 \end{cases} \qquad \hat{A}_{i+1/2}^{n} = 0.5 \cdot \left(A_i^n + A_{i+1}^n\right)$$

The source term $S_{i+1/2}$ is described in detail in section 3.4.

The continuity equation is implicit and reads:

$$A_i^{n+1} = A_i^n - \frac{\Delta t}{\Delta x_i}\left(Q_{i+1/2}^{n+1} - Q_{i-1/2}^{n+1}\right)$$

6.2 *ONE-Dimensional Dam-Break Simulation Codes*

6.2.1 SMPDBK Simplified Dam Break Model

This model was developed by Wetmore and Fread (1984) at the National Weather Service (NWS) of the USA.

The NWS SMPDBK model computes the dam break outflow from a simplified equation and routes the outflow based on curves generated with the NWS DAMBRK model. Flow depths are computed based on Manning's equation.

The SMPDBK model can quikly be processed with a minimal amount of data. It can generate the dam-break floodwave peak flows, peak flood elevations, and peak travel times at selected downstream points.

6.2.2 DAMBRK

This DAMBRK model was developed at the National Weather Service (NWS) of the USA.

The governing equations of the model are the complete De Saint-Venant equations which are coupled with internal boundary equations representing the rapidly varied (broad-crested weir) flow through structures. In addition, suitable external boundary equations at the upstream and downstream ends of the routing reach are utilized. The system of equations is solved by a non-linear weighted four-point implicit finite-difference method.

The finite difference scheme of this code was developed by Pressman (Cunge et al. 1980).

It is valid only for subcritical flows, while it has been demonstrated to be instable for supercritical flows. Some numerical tricks allow using it also for slightly supercritical flows. The breach module of the computer code describes the temporal and geometrical dam breach and it also determines the resulting water surface elevations and flood-wave travel times.

6.2.3 CASTOR

This is a simplified dam-break wave model which uses the uniform-flow equation to compute peak water elevation, peak velocity, and wave arrival time.

The main feature of the model is that the computation at a given section doesn't use the data of other sections but it only depends on local data, distance from the dam, Manning roughness coefficient between the dam and the section and some initial data of the dam and the reservoir.

A comparison of CASTOR results with a solver of De Saint-Venant equations shows that the deviation of the peak water depths is less than 20% except for points of rapid topographic change. (Paquier et al. 1997).

6.2.4 HEC-RAS

The Hydrologic Engineering Center (HEC) in Davis, California developed the River Analysis System (RAS) for the US Army Corps of Engineers and public released the software in 1995.

HEC-RAS is a computer program for modeling water flowing through systems of open channels and computing water surface profiles. HEC-RAS finds particular commercial application in floodplain management and flood insurance studies to evaluate floodway encroachments. It can be used for dam breach analysis, though other modeling methods are presently more widely accepted for this purpose. Figure 21

HEC-RAS solves the water shallow equations in a non-conservative form.

Despite HEC-RAS has the advantage of being accepted by many government agencies and private firms, the numerical methods used are obsolete so that the software experiences instability problems during mixed flow regimes (transcritical flows) and flow discontinuities. This issue is the same presented by DAMBRK code because they both use the Pressman numerical scheme.

The shallow water equations in this non-conservative form are not suitable for solving dam break type flows with these features.

HEC-RAS deals with mixed flow regimes changes the nature of the equations solved.

In order to deal with the stability problems resulting from the presence of mixed flow regimes Fread (1986), the developer of HEC-UNET (which later become the unsteady flow solver for HEC-RAS), has introduced a concept call the "Local Partial Inertia Technique (LPI)". This method is implemented in HEC-RAS as an option for solving mixed flow regime problems.

The LPI methodology consists of using a multiplier in front of the first two terms (inertia terms) which reduces their contribution as the Froude number approaches to 1 (critical flow).

It is important to note that the LPI is nothing but a procedure that converts the full-dynamic unsteady momentum equation (SWE) into a diffusive flow equation, by getting rid of the inertia terms, as the Froude number of the flow approaches to 1 (critical flow).

HEC-RAS does not contain any consideration regarding the wet-dry fronts, or flow discontinuities. Any flow discontinuities are completely smeared. Due to these shortcomings, the unsteady flow option of HEC-RAS may be subject to numerical instabilities under some flow conditions.

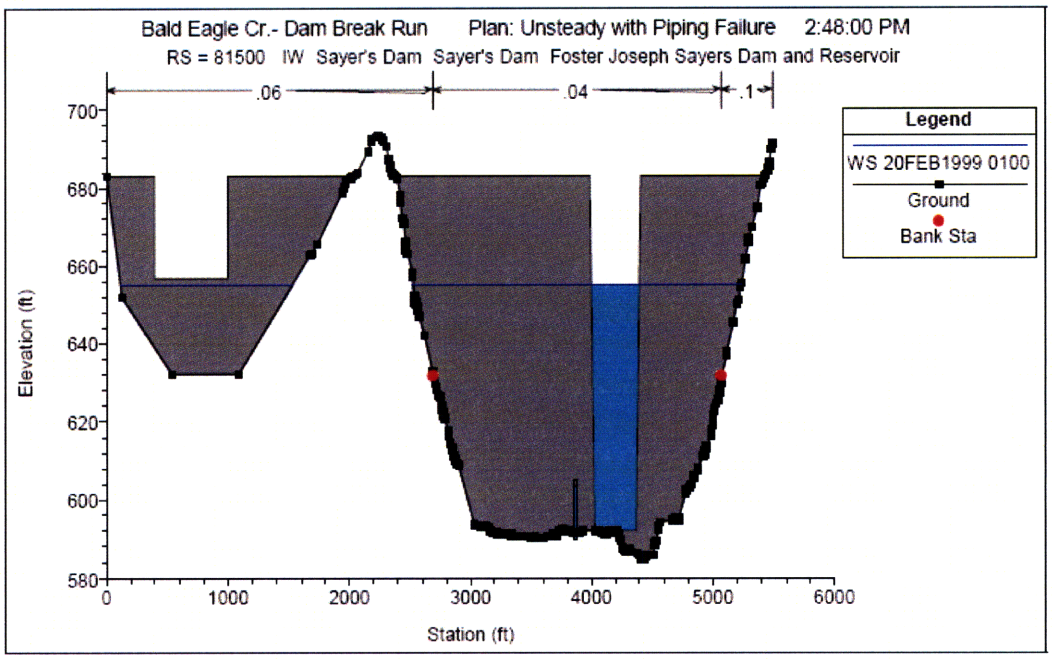

Figure 21- Example HEC-RAS plot of dam while breaching. (ASCE 2004).

6.3 Comparisons of Dam-Break Simulation Codes

6.3.1 SMPDBK vs. DAMBRK

Bozkuş et al. (1998) compared three numerical failure simulations of the same dam employing the numerical models NWS SMPDBK and DAMBRK and the physical experimental measurements. Comparisons of the measured and computed results indicate that both numerical models predict the peak flood elevations with reasonable accuracy. As expected the results of the more sophisticated model DAMBRK were more accurate than those of SMPDBK, which underestimated the peak water elevations.
Figure 22).

In general, the DAMBRK model is best suited for pre-emergency dam-break analyses since it requires detailed input data for an accurate analysis, as well as technical expertise to use it. On the other hand, the SMPDBK model was better suited for real-time predictions of the behaviour of dam-break flood waves in the cases where a dam-failure is imminent and there is not sufficient time for a

comprehensive dam-failure analysis. It is worthy to note that the latter use of a dam-break code is obsolete.

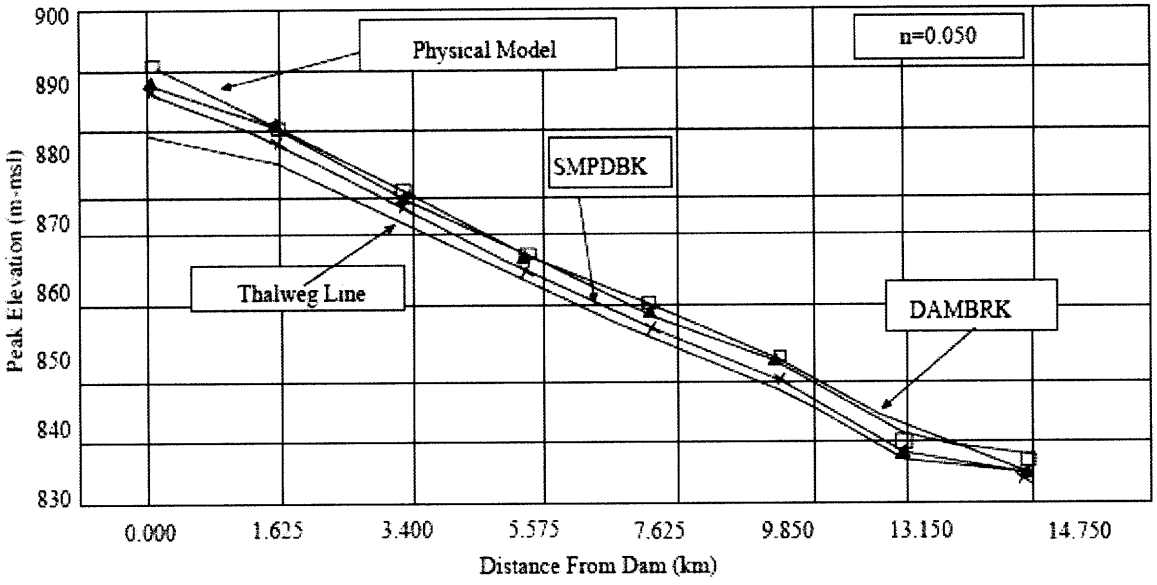

Figure 22- Comparison of peak water surface elevation vs. distance downstream. (Bozkuş et al. 1998).

6.3.2 HEC-RAS vs. ORSA

While HEC-RAS code integrates Shallow Water Equations (SWE) written in non conservative form, ORSA adopts two different finite volumes solvers to integrate SWE: Roe scheme and a modified Lax - Friedrichs scheme.

As aforementioned, HEC-RAS introduces a numerical filter, limiting the convective inertia term, to overcome the problem of instability when the flow becomes supercritical.

The models are compared simulating a 200 years return period flood wave propagation for a river characterized by sudden variations of cross section width. (Natale et al. 2007).

The results indicate that HEC-RAS doesn't reproduce the frequent flow regime transitions of the river and becomes unstable unless an artificial magnifying of Manning roughness coefficient. The unlikeness of results (
Figure 23), are mostly due to the different method of spatial interpolation of the two codes.

Water depths computed by HEC-RAS are significantly greater than those computed by ORSA code. The evidence is substantial for floodplains, where the valley is essentially flat.

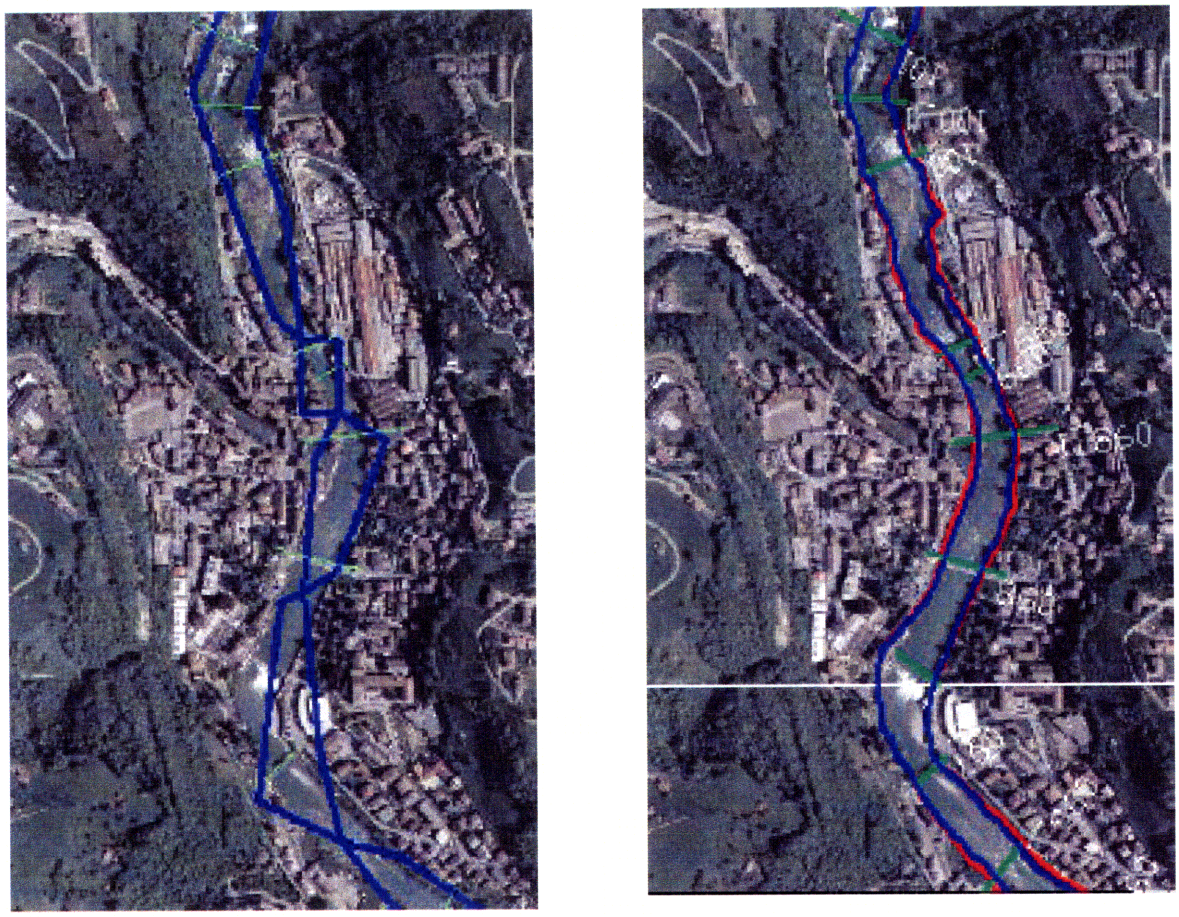

Figure 23- On the left is showed the perimeter obtained using HEC-RAS w/o modifying the resistance coefficients. On the right it is showed the HEC-RAS perimeteration after the elimination of some transitional sections and increasing the Manning coefficients. The red line shapes the ORSA flood prone area.

6.4 Case Studies of Dam Failure: comparison of breach predictions

6.4.1 Simulation of the Big Bay Dam failure

The Big Bay Dam embankment failure occurred on March 12, 2004, 12 years after construction. This lake is located 11 miles west of Purvis, Mississippi on Bay Creek Road in Lamar County. The dimensions of the dam were approximately 576 m of length and 15.6 m of height. The release of water consequent to the failure was

approximately 17,500,000 m^3 inundating 23 km of valley to depths of up to 10.0 m until the Pearl River.

The capabilities of a HEC-RAS unsteady flow model were assessed comparing the high water levels predicted by the modelling with measured high water marks.

HEC-RAS results were relatively accurate but some random errors showed the geometry extracted from the 10-m DEM introduced measurable mistakes to the analysis.

Nevertheless HEC-RAS underpredicted the value of the peak break flow, it is considered the best modelling estimate of it. Other National Resources Conservation Service models were used: WinTR-20 results compared reasonably well with the high water marks for this failure. TR-66 results did not compare well, only providing a solution for a short and insufficient distance downstream and overpredicting attenuation.

6.4.2 Simulation of the St. Francis Dam failure

Saint Francis Dam was a curved concrete dam constructed between 1924 and 1926 under the direction of Chief Engineer and Manager William Mulholland. The dam was situated in San Francisquito Canyon, California. The dimensions of the dam were 57 m of height and 213 m of length. It could store roughly 47 million m^3 of water. The dam failure occurred on March 12, 1928, because it was built on and with a poor foundation. The simulation presented by Begnudelli and Sanders (2007) is evaluated using flood arrival time data (Outland 1963) and flood inundation maps (Rogers and James 2003).

The a priori travel time prediction, high-resolution digital elevation models for terrain data (USGS 2006), an open-source mesh generation tool, and a modern dam-break flooding algorithm based on a Godunov-type finite volume scheme to integrate SWE enabled to build an accurate two-dimensional 2D dam-break model.

The most accurate predictions are achieved with a uniformly distributed Manning n=0.02. A 50% increase in the Manning coefficient had little effect on the prediction of flooded area but degraded the accuracy of arrival time predictions to 25% by slowing the speed of the flood.

Certainly the model accuracy must be partly attributed to knowledge of the reservoir volume at the time of failure. In a predictive modelling it should be taken into account that this would represent another source of uncertainty.

Additionally the study underlines the importance of a dynamic momentum balance for dam-break flood simulation.

References

Altinakar, M., "Working Group on Dam Issues Related to Floodplain Management.", November 11, 2008.

Bajracharya, B., Shrestha, A. B., and Rajbhandari, L., (2007). "Glacial Lake Outburst Floods in the Sagarmatha." *Mountain Research and Development*, 27 (4) , 336–344.

Begnudelli, L; Sanders, BF (2007). "Simulation of the St. Francis Dam-Break Flood." *J. Eng. Mech.*, 133(11), 1200-1212.

Bozkuş, Z., and Kasap, A. (1998). "Comparison of Physical and Numerical Dam-Break Simulations." *Tr. J. of Engineering and Environmental Science*, 22, 429- 443.

Burguete, J., and García-Navarro, P. (2001). "Efficient construction of high-resolution TVD conservative schemes for equations with source terms: Application to shallow water flows." *Int. J. Numer. Methods Fluids*, 37, 209–248.

Cenderelli, D. A., Whol, E. E., (2003). "Flow hydraulics and geomorphic effects of glacial-lake outburst floods in the mount Everest region, Nepal." *Earth Surf. Process. Landforms* 28, 385–407.

Central Intelligence Agency (CIA) (2008). Chile. "The World Factbook." Retrieved November 30, 2008 from https://www.cia.gov/library/publications/theworldfactbook/geos/ci.html.

Cunge, J.A., Holly, F.M., Verwey, A. (1980). Practical Aspects of Computational River Hydraulics. Pitman, London.

Engineering and Design - Hydrologic Engineering Requirements for Reservoirs. (1997). *USACE*. EM 1110-2-1420, Chapter 16.

Froehlich, D. C. 1995(b). "Embankment Dam Breach Parameters Revisited." *Journal of Water Resources Planning and Management*, **121**(1), 90-97.

Garcia-Navarro, P. et al. (1999). "Dam-break flow simulation: some results for one-dimensional models of real cases." *Journal of Hydrology*, 216, 227–247.

García-Navarro, P., and Vázquez-Cendón, M. E. (1999). "On numerical treatment of the source terms in the shallow water equations." *Comput. Fluids*, 29, 185–210.

Guidelines for Failure Impact Assessment of Water Dams (2002). *The State of Queensland, Department of Natural Resources and Mines*

Hubbard, M. E., and García-Navarro, P. (2000). "Flux difference splitting and the balancing of source terms and flux gradients." *J. Comput. Phys.*, 165, 89–125.

Natale, L., Petaccia, G., Savi, F., Zanotti, M., (2007). "Mapping of flood risk prone areas: a comparison between different models and techniques." *Geophysical Research Abstracts*, 9, 06704.

Outland, C. F. (1963). "Man-made disaster: The story of St. Francis Dam." The Arthur H. Clark Company.

Pabich, W.J. (2008). Request for Proposal. Massachusetts Institute of Technology, Department of Civil and Environmental Engineering.

Paquier, A., and Robin, O., (1997). "CASTOR: Simplified Dam-Break Wave Model." *Journal of Hydraulic Engineering*, 123(8), 724-727.

Petteri, A., and Juha Aaltonen, J., (2007). "Comparing a 1D hydraulic model with a 2D hydraulic model for the simulation of extreme glacial outburst floods." *Hydrol. Process.* 22, 1537–1547.

Pérez, G. et al. (2006). "One-Dimensional Model of Shallow Water Surface Waves Generated by Landslides." *J. Hydraulic Eng.*, 132 (5), 462-473.

Ritter, A. (1892). "Die Fortpflanzung der Wasserwellen". *Zeitschrift des Vereins Deutscher Ingenieure* 36 (33), 947 – 954.

Roe P.L. (1981). "Approximate Riemann solvers, parameter vectors, and difference schemes." *Reprinted from the Journal of Computational Physics*, 43, 357-372.

Rogers, J. D., and James, K. (2003). "Mapping the St. Francis Dam outburst flood with geographical information systems." *Proc., 46th Annual Meeting of the Association of Engineering Geologists*, Vail, Colo., 72, (http://web.umr.edu/~rogersda/st_francis-dam).

Strikwerda, J.C. (1989). "Finite Difference Schemes and Partial Differential Equations." Wadsworth & Brooks/Cole, Pacific Grove, CA.

Strittholt, J. R. (2008). "Potential Ecological Impacts from Proposed Hydroelectric Projects on the Baker and Pascua Rivers in the Aisen Region of Patagonia Chile." Conservation Biology Institute.

Von Thun, J. L., and D. R. Gillette, (1990). "Guidance on Breach Parameters." unpublished internal document, U. S. Bureau of Reclamation, Denver, Colorado, March 13, 1990, 17.

Yochum, SE; Goertz, LA; Jones, PH (2008). "Case Study of the Big Bay Dam Failure." *J. Hydraul. Eng.*, 134(9), 1285-1293.

ACKNOWLEDGEMENTS

To my Father, a modern Socrates, deep connoisseur of the Maieutic Art.

To my sweet Mother, which gave me birth.

To my brother Giulio and my wonderful Grandma.

To my irreplaceable friends Discy e Nicola, so far away but always so close to me.

To the great friends I met in my wonderful experience at MIT; in particular I'm grateful to my very best friend Diego, source of support and laughs.